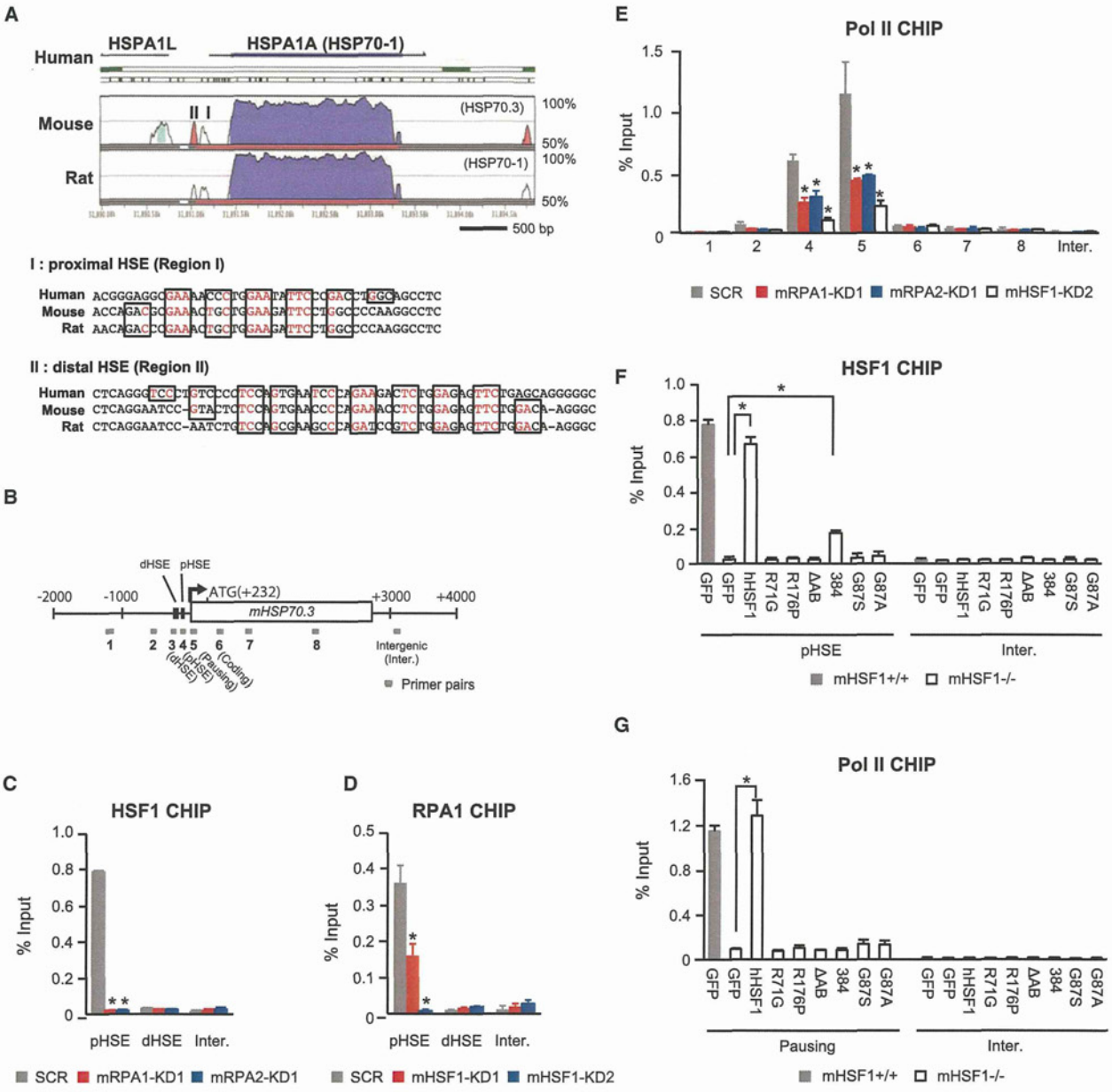

Figure 2. RPA Is Required for HSF1 Access to HSP70 Promoter and Pol II Preloading

(A) Alignment of sequences of human *HSPA1A* gene with those of mouse and rat orthologous genes. Genomic sequences were aligned with the VISTA program (http://genome.lbl.gov/vista/index.shtml), and percent identity is shown (upper). The proximal and distal HSEs are located in conserved promoter regions I and II, respectively (lower). Consensus nGAAn units are boxed, and conserved sequences are highlighted in red.

(B) Schematic representation of mouse HSP70.3 locus. Amplified DNA regions by real-time PCR are shown as numbered gray boxes.

(C) HSF1 constitutively binds to pHSE. MEF cells were infected with adenovirus expressing each shRNA, and ChIP analyses were performed using HSF1 antibody.

(D) RPA1 is recruited to the pHSE. MEF cells were infected with adenovirus expressing each shRNA, and ChIP-qPCR analyses were performed using RPA1 antibody.

(E) Pol II recruitment to the mouse HSP70.3 locus. MEF cells were infected with adenovirus expressing each shRNA, and ChIP-qPCR analyses were performed using Pol II antibody.

(F) Binding of hHSF1 mutants to HSP70 promoter. Wild-type hHSF1, each hHSF1 mutant, or GFP was expressed in wild-type (HSF1+/+) or HSF1 null (mHSF1−/−) MEF cells. ChIP-qPCR analyses of pHSE or an intergenic region were performed using HSF1 antibody.

(G) Recruitment of Pol II in the presence of hHSF1 mutants. MEF cells were treated as described in (F). ChIP-qPCR analyses of pausing and intergenic regions were performed using Pol II antibody. Error bars, SD (n = 3) in (C)–(G). Asterisks indicate $p < 0.01$ by Student's t test in (C)–(G) (see also Figure S3).

upon PCNA knockdown (Figure S3C). RPA1 was also recruited to pHSE only in the presence of HSF1 (Figure 2D). Even though one was overexpressed, it was unable to occupy pHSE without the other (Figures S3D and S3E). These results indicate that HSF1-RPA complex formation is indispensable for HSF1 access to pHSE in vivo in unstressed cells. In contrast, in heat-shocked cells, HSF1 bound not only to pHSE but also to dHSE, and knockdown of RPA1 partially reduced HSF1 binding to both HSEs only at an early step during heat shock (Figure S3F). It is unclear why HSF1 binds to only pHSE under control condition, but HSF1-RPA complex might be stabilized in this site in vivo. Thus, HSF1-RPA complex constitutively accesses to the HSP70 promoter in vivo, which is required for rapid induction of HSF1 binding in response to heat shock.

HSF1-RPA Complex Is Required for Pol II Preloading

Pol II is preloaded in the promoter-proximal region of the *Drosophila HSP70* gene prior to heat shock (Gilmour and Lis, 1985); therefore, we examined whether constitutive HSF1 access to the HSP70 promoter is associated with Pol II preloading in mammalian cells. We found that levels of Pol II preloading before stimulation are significantly reduced in the pausing region of HSP70 promoter by knockdown of *RPA1*, *RPA2*, or *HSF1* (Figure 2E). To find a region of HSF1 that is required for Pol II preloading, we replaced endogenous HSF1 with its mutant by infecting HSF1 null MEF cells with adenovirus expressing each mutated HSF1 (Figures S3G and S3H). The pHSE of HSP70 promoter was not bound by HSF1 mutants that were unable to bind to HSEs (HSF1R71G) (Inouye et al., 2003), form trimers (HSF1R176P, HSF1ΔAB) (Inouye et al., 2007), or interact with RPA1 (HSF1G87S, HSF1G87A) (Figure 1E); moreover, Pol II loading was not induced by any aforementioned mutant (Figures 2F and 2G). In contrast, an HSF1 mutant lacking an activation domain (HSF1-384) (Shi et al., 1995; Zuo et al., 1995; Green et al., 1995) did bind to pHSE, but was unable to induce Pol II loading. Thus, both the DNA-binding activity of HSF1 and its interaction with RPA1 are required for its access to pHSE in vivo, and the activation domain is required for the regulation of Pol II preloading, but not for access.

HSF1-RPA Complex Opens the Chromatin Structure of HSP70 Promoter

The access of transcription factors may actively open the chromatin structure and facilitate the binding of other factors at the promoter region. Therefore, we next examined histone occupancy and chromatin marks on the HSP70 promoter. Under unstressed condition, the occupancy of histones H2B and H3 was much lower on the nucleosome-depleted HSP70 promoter in MEF cells than on the gene body, and occupancy was significantly increased by knockdown of *HSF1* as well as *RPA1* or *RPA2* (Figure 3A). Furthermore, active chromatin marks, H3K4 trimethylation, and H3K27 and H3K9 acetylation were reduced by knockdown of *RPA1* or *RPA2*, whereas an inactive mark, H3K9 trimethylation, was increased (Figure 3B). Re-expression of human HSF1 restored the increased histone H3 occupancy and reduced active chromatin marks, whereas re-expression of hHSF1G87S or hHSF1G87S did not (Figures 3C and 3D), indicating the requirement of HSF1-RPA1 interaction. Taken together, HSF1-RPA1 complex opens the chromatin structure of HSP70 promoter.

We noticed that the histone occupancy in HSP70 promoter after knockdown of HSF1 or RPA did not recover to the level of that in its gene body (Figure 3A). It was reported previously that SP1 and NF-Y binding sites in human HSP70 promoter are occupied in vivo under control condition (Figure S4A) (Abravaya et al., 1991) and are involved in basal transcription (Wu et al., 1986; Morgan et al., 1987; Greene et al., 1987). We found that the occupancy of both SP1 and NF-YB is significantly reduced by knockdown of HSF1 or RPA1 (Figure S4B). Occupancy of SP1 and NF-YB also depends on each other (Figure S4C). Furthermore, knockdown of SP1 or NF-YB reduced the occupancy of HSF1-RPA complex, Pol II preloading, and active chromatin marks (Figure S4D). These results suggest that the chromatin structure of HSP70 promoter is opened not only by the HSF1-RPA complex but also together with other factors such as SP1 and NF-Y (Duan et al., 2001; Goodwin et al., 2001), which might play a role similar to *Drosophila* GAGA factor.

To confirm that the effects of RPA1 knockdown might be specific to HSF1-target promoters, we examined its effects on the promoters of SP1- or NF-YB-target genes, whose expression was specifically downregulated by each knockdown (Figure S4E). Knockdown of RPA1 did not affect the recruitment of SP1 or NF-YB on the promoter of each target gene, occupancy of Pol II and histone H3, and an active chromatin mark (Figures S4F and S4G). These results emphasize the specific role of RPA1 in HSF1-mediated chromatin opening.

HSF1-RPA Complex Recruits FACT, which Displaces Histones

We asked how HSF1-RPA complex gains access to nucleosomal DNA and opens the chromatin structure. Because ssDNA-binding proteins could modulate transcription by interacting with a single-stranded nontemplate strand of Pol II complex during transcription (Sikorski et al., 2011), we first examined the roles of the ssDNA-binding activity of RPA complex by using RPA1 mutants lacking its activity (Figures S5A and S5B) (Haring et al., 2008). Interestingly, the substituted amino acids were located in the HSF1-interacting region, and RPA1TM and RPA1F269A interacted with HSF1, whereas RPA1AroA did not and RPA1F238A did only a little (Figures 4A and 4B). Replacement of endogenous RPA1 with RPA1TM lacking only ssDNA-binding activity had no effect on HSF1 binding to pHSE of HSP70 promoter or on Pol II preloading in human HeLa cells, whereas that with RPA1AroA abolished the occupancy of HSF1 and Pol II (Figures 4C, 4D, and S5C–S5E). These results suggest that ssDNA-binding activity of RPA1 is dispensable for HSF1 access to nucleosomal DNA in vivo.

It was shown previously that yeast RPA interacts with a component of a histone chaperone complex FACT, which displaces the histone H2A-H2B dimer (VanDemark et al., 2006). Both FACT and HSF are recruited to heat shock loci during heat shock in *Drosophila* (Saunders et al., 2003). Therefore, we next examined its involvement in the access of HSF1-RPA complex to nucleosomal DNA. Mammalian FACT complex is composed of two subunits, SPT16 and SSRP1 (Avvakumov et al., 2011). We found that SPT16 is coprecipitated with

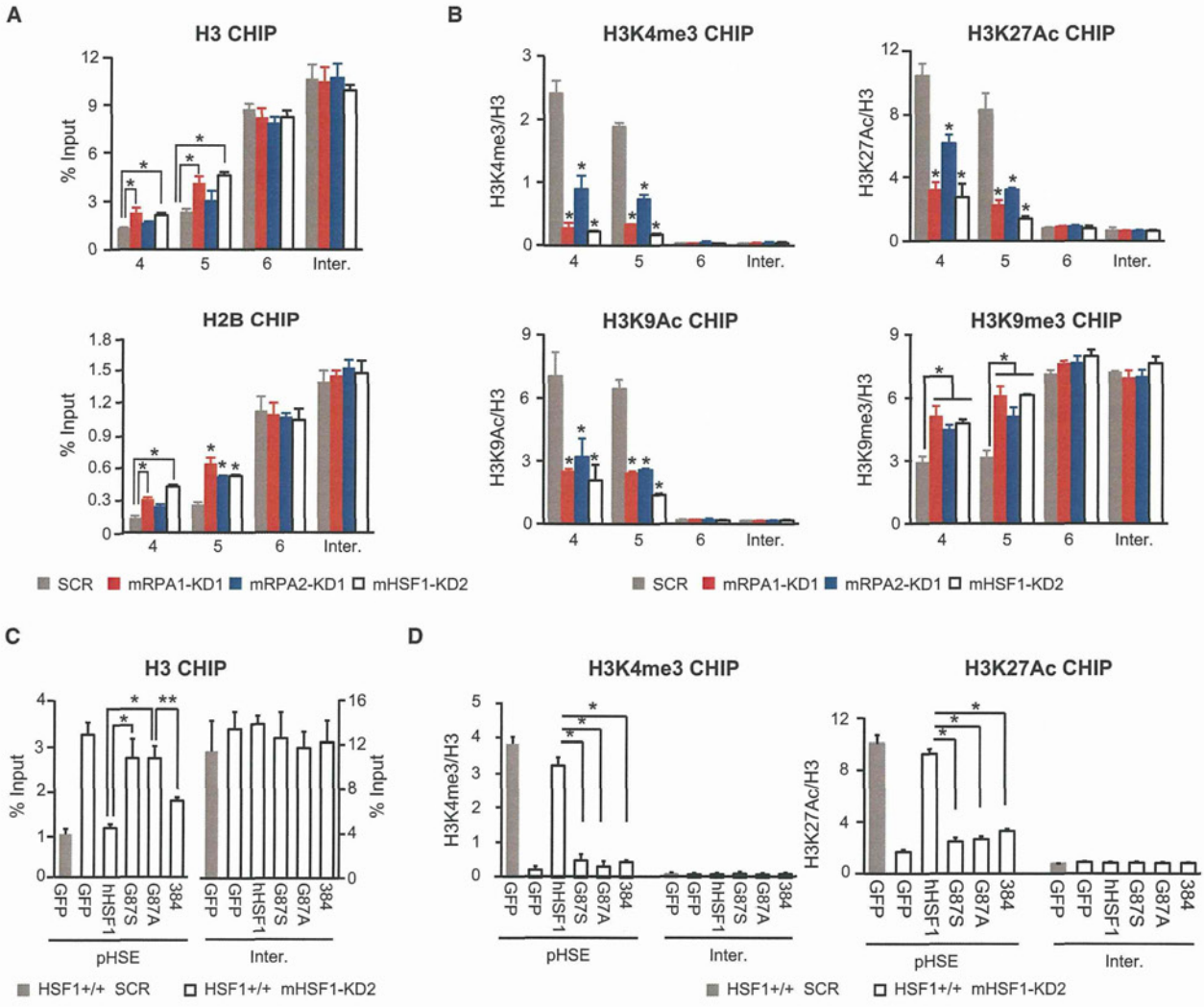

Figure 3. HSF1-RPA Complex Opens Chromatin Structure of HSP70 Promoter

(A) Histone occupancy. MEF cells were infected with adenovirus expressing each shRNA for 72 hr. ChIP-qPCR analyses were performed using H2B or H3 antibody.

(B) Levels of active and inactive chromatin marks. MEF cells were treated as described in (A), and ChIP-qPCR analyses were performed. Levels of H3K4 trimethylation, H3K27 and H3K9 acetylation, and H3K9 trimethylation in different regions of HSP70 locus were normalized to histone H3 occupancy.

(C) Histone occupancy in MEF cells expressing each hHSF1 mutant. Cells were infected with Ad-sh-mHSF1-KD2 or Ad-sh-SCR as a control and were then infected with adenovirus expressing each hHSF1 mutant or GFP. ChIP-qPCR analyses of the pHSE and intergenic regions on the mouse HSP70 locus were performed using H3 antibody.

(D) Levels of active chromatin marks in cells expressing each hHSF1 mutant. Cells were treated as described in (C), and levels of H3K4 trimethylation and H3K27 acetylation were normalized to histone H3 occupancy. Error bars indicate SD (n = 3), and asterisks $p < 0.01$ by Student's t test in (A)–(D) (see also Figure S4).

wild-type RPA1 and all RPA1 mutants lacking both ssDNA-binding activity and the ability to interact with HSF1 (RPA1AroA and HSF1F238A) or only ssDNA-binding activity (RPA1TM) (Figure 4E). We used ChIP assay to show that SPT16 is recruited to the pHSE but not to the dHSE of HSP70 promoter in unstressed MEF cells, and knockdown of RPA1 or HSF1 abolished SPT16 recruitment (Figure 4F). Furthermore, knockdown of SPT16 reduced RPA1 recruitment and Pol II preloading and increased the occupancy of histone H2B (Figures 4G–4I). These results indicate that HSF1-RPA complex gains access to nucleosomal DNA partly through the recruitment of FACT, which displaces histones.

RPA1 Is Required for HSF1-Mediated Gene Expression

To examine whether HSF1-RPA complex regulates the expression of genes other than *HSPs*, we performed DNA microarray analysis. The expression of 564 genes decreased by more than 1.3-fold ($p < 0.05$) in HSF1-knockdown MEF cells, and that of

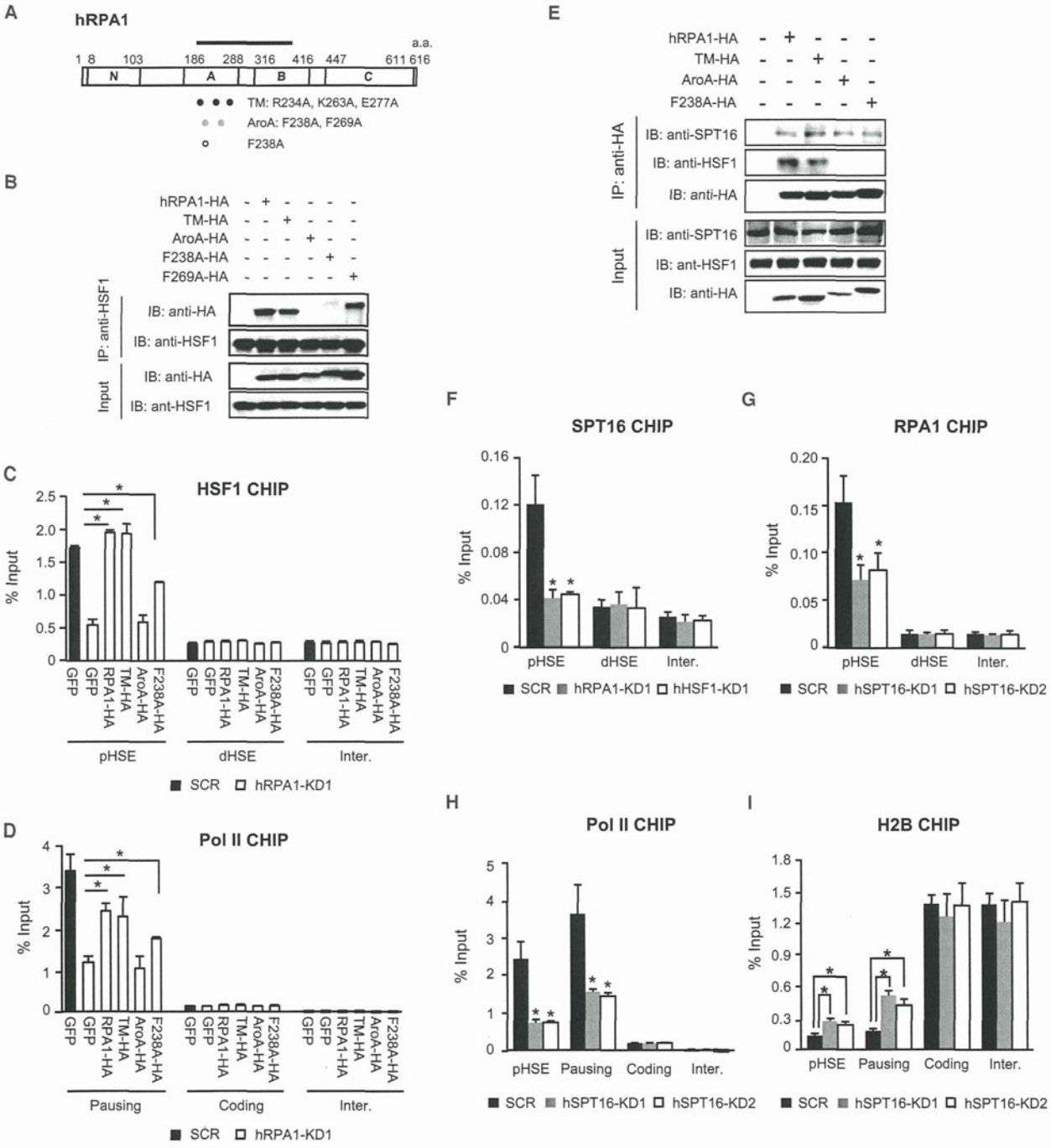

Figure 4. HSF1-RPA Complex Recruits FACT, which Displaces the H2A-H2B Dimer

(A) Schematic representation of RPA1 mutants lacking ssDNA-binding activity. hRPA1-TM shows substitution of three amino acids (black circles) with alanine, and hRPA-AroA shows substitution of two amino acids including F238 and F269 (gray circles) with alanine. A bar indicates an HSF1-interaction domain.

(B) Interaction of HSF1 with RPA1 mutants. HEK293 cells were transfected with an expression vector for wild-type or mutated hRPA1-HA. Proteins coimmunoprecipitated with endogenous HSF1 were subjected to western blotting.

(C and D) HSF1 binding and Pol II recruitment in the presence of RPA1 mutants. Endogenous RPA1 was depleted by knockdown and was replaced with each hRPA1 mutant or GFP in HeLa cells. ChIP-qPCR analyses of indicated regions in the human HSP70-1 locus were performed using HSF1 antibody.

(E) SPT16 interacts with RPA1 or its mutants independently of HSF1. HEK293 cells were transfected with an expression vector for wild-type or mutated hRPA1-HA. Proteins coimmunoprecipitated using HA antibody were subjected to western blotting.

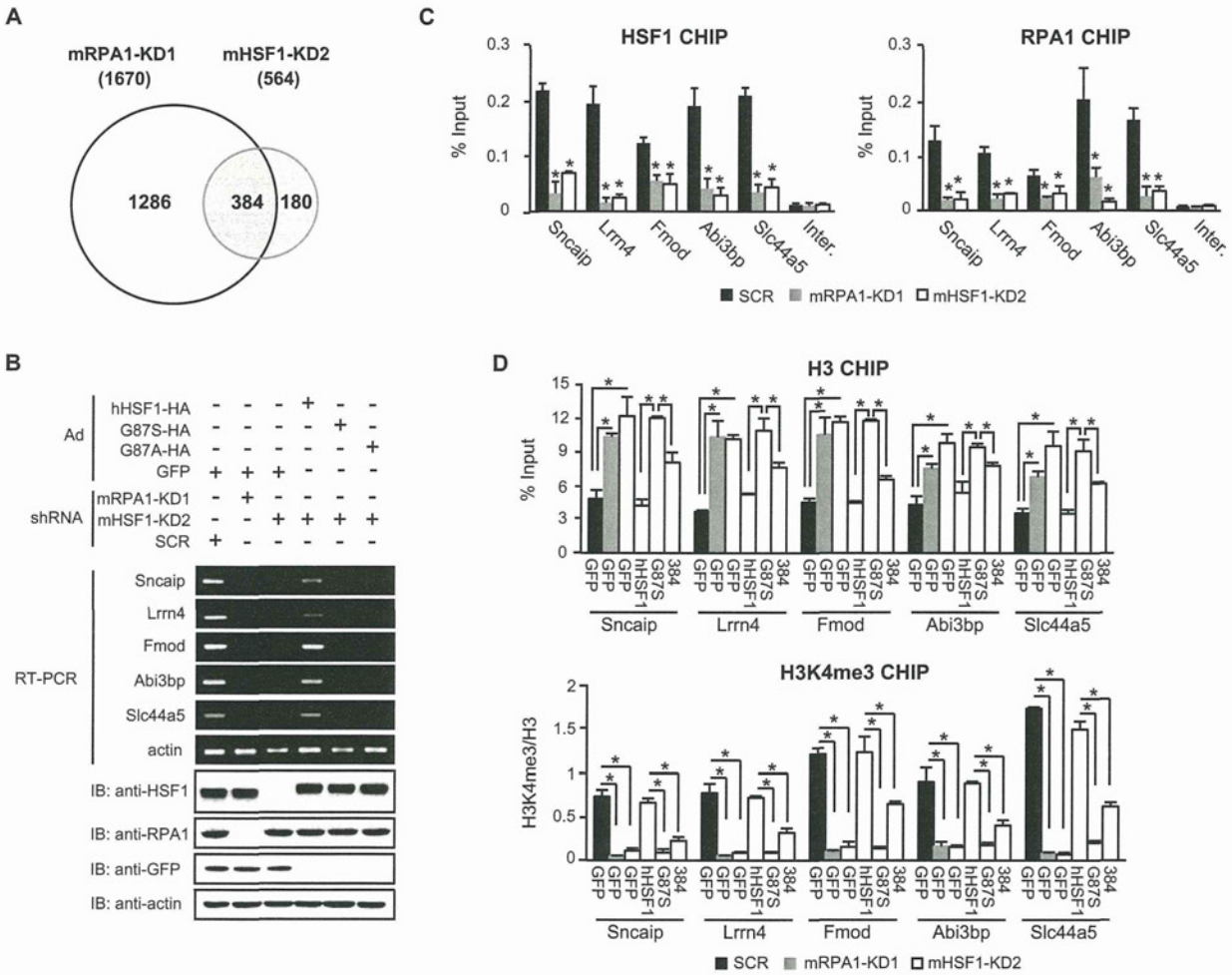

Figure 5. RPA Is Required for Basal Expression of HSF1-Target Genes

(A) Venn diagram showing genes downregulated by knockdown of RPA1 or HSF1 and their overlap. Microarray analysis was performed in MEF cells infected with Ad-sh-mHSF1-KD2, Ad-sh-mRPA1-KD1, or Ad-sh-SCR as a control. Overall, 1,670 and 564 genes showed more than a 1.3-fold decrease ($p < 0.05$ by Student's t test, $n = 3$) by knockdown of mRPA1 and mHSF1, respectively.

(B) Expression of the target genes by wild-type hHSF1, hHSF1-G87S, or hHSF1-G87A. Endogenous HSF1 was depleted by knockdown and was replaced with each hHSF1 mutant in MEF cells. RT-PCR was performed (upper). Levels of wild-type and mutated hHSF1 were examined by western blotting (lower).

(C) HSF1 and RPA1 occupancy of HSEs on targets after knockdown of RPA1 or HSF1. MEF cells were infected with adenovirus expressing each shRNA. ChIP-qPCR analyses were performed using HSF1 or RPA1 antibody.

(D) Chromatin opening by wild-type hHSF1, but not by hHSF1-G87S or hHSF1-384. MEF cells were treated as described in (C). ChIP-qPCR analyses were performed using antibody for H3 and H3K4 trimethylation. Error bars indicate SD ($n = 3$), and asterisks $p < 0.01$ by Student's t test in (C) and D (see also Figure S6).

1,670 genes did so in RPA1-knockdown cells (Figure 5A). The expression of 384 genes (68%) of the downregulated genes by HSF1 knockdown was simultaneously decreased by RPA1 knockdown, suggesting them to be common target genes. Among markedly downregulated genes, we examined five randomly selected genes, *Sncaip*, *Lrrn4*, *Fmod*, *Abi3bp*, and *Slc44a5*, in more detail (Figures S6A and S6B). Reduced expression of these genes after HSF1 knockdown was restored by re-expression of wild-type HSF1, but not by expression of HSF1G87S or HSF1G87A (Figure 5B). ChIP assay showed that

(F) Recruitment of SPT16 to the pHSE requires HSF1-RPA complex. HeLa cells were infected with adenovirus expressing each shRNA. ChIP-qPCR analyses of pHSE, dHSE, and intergenic regions in the human HSP70-1 locus were performed using SPT16 antibody.

(G–I) SPT16 knockdown decreases RPA1 recruitment, Pol II preloading, and histone occupancy. HeLa cells were infected with adenovirus expressing each shRNA. ChIP-qPCR analyses on indicated regions were performed using RPA1, Pol II, or H2B antibody. Error bars indicate SD ($n = 3$), and asterisks $p < 0.01$ by Student's t test in (C), (D), and (F)–(I) (see also Figure S5).

both HSF1 and RPA1 were occupied in the promoters of these genes and occupancy of one depended on the other (Figure 5C). Furthermore, analysis of histone occupancy and active chromatin marks revealed that HSF1-RPA1 complex opened their chromatin structure (Figures 5D and S6C). Among five genes, the expression of *Sncaip* and *Abi3bp* was moderately induced during heat shock, but was not induced at all by RPA1 knockdown (Figure S6D). Taken together, HSF1-RPA complex regulates the expression of many *non-HSPs* as well as *HSPs* under control condition in the same manner as it regulates *HSP70* expression.

HSF1-RPA Complex Supports Melanoma Cell Proliferation

Downregulation of HSF1 targets, including *HSP* and *non-HSP*, may be associated with reduced proteostasis capacity (Hayashida et al., 2010). In fact, MEF cells were more sensitive to heat shock by substitution of wild-type HSF1 with HSF1G87S or G87A (Figures S7A and S7B), and an aggregation-prone polyglutamine protein formed more aggregates in cells where wild-type HSF1 was replaced with the interaction mutants (Figure S7C). Furthermore, we noticed that 8 of 33 genes, which were downregulated more than 2-fold ($p < 0.05$) by HSF1 or RPA1 knockdown, were related to cancer (Figure S6A). Therefore, we examined the impact of HSF1-RPA complex on the proliferation of human melanoma HMV-1 and MeWo cells (Nakamura et al., 2010). This revealed that reduced proliferation of HSF1-knockdown cells was restored by overexpression of wild-type HSF1 but not by that of the interaction mutant, HSF1G87S or HSF1G87A, in culture dishes (Figures 6A, 6B, and S7D). We next performed xenograft experiments in which athymic nude mice were injected subcutaneously with HMV-1 cells, where wild-type HSF1 was replaced with each HSF1 mutant. The tumor formation of HMV-1 cells harboring one of the interaction mutants was significantly reduced compared with those harboring wild-type HSF1 (Figures 6C, 6D, and S7E). These results demonstrate that HSF1-RPA complex is required for melanoma cell proliferation as well as the maintenance of proteostasis.

DISCUSSION

DNA is strongly associated with histone proteins, and this structure, termed "nucleosome," prevents transcription factor access to the DNA elements. This nucleosome arrangement is fluid, and nucleosomal DNA is transiently unwrapped in vitro (Li et al., 2005). Therefore, transcription factors can bind to cognate DNA elements, but are quickly removed by histones in the absence of a stabilizing mechanism. Nucleosome arrangement in vivo is further regulated by chromatin remodeling factors, histone-modifying enzymes, and histone chaperones, which make it more fluid (Kingston and Narlikar, 1999; Avvakumov et al., 2011). It is speculated that transcription factors may access nucleosomal DNA by recruiting these factors in a cooperative manner (Li et al., 2007). This study unexpectedly established that HSF1 access to nucleosomal DNA requires its interaction with RPA, which plays a major role in DNA replication and repair. This HSF1-RPA complex recruits not only a chromatin-remodeling complex containing BRG1, which interacts with an HSF1-activation domain (Sullivan et al., 2001; Fan et al., 2003), but also a histone chaperone, FACT, which interacts with RPA. Knockdown of FACT or BRG1 partially reduced the occupancy of HSF1 and RPA1 on HSF70 promoter (Figure 4G, data not shown). Thus, we propose that HSF1-RPA complex gains access to nucleosomal DNA in part by recruiting FACT, probably in cooperation with a chromatin-remodeling complex containing BRG1 (Figure 6E).

RPA is a heterotrimeric, single-strand DNA-binding protein required for DNA metabolism, including DNA replication, repair, and recombination. It not only protects ssDNA from nucleases and prevents hairpin formation in ssDNA during DNA processing, but also recruits a variety of DNA processing proteins through direct interaction (Fanning et al., 2006). In addition, RPA is suggested to be involved in gene transcription. First, RPA was found to bind to human metallothionein promoter (Tang et al., 1996). Second, nucleotide excision repair factors including RPA were localized in human active promoters (Le May et al., 2010). Third, RPA and another ssDNA-binding protein, Sub1, were associated with Pol II in yeast, suggesting their interaction with the nontemplate strand of Pol II complex during transcription (Sikorski et al., 2011). We here show a mechanism in which RPA supports transcription factor access to nucleosomal DNA as a scaffold for HSF1 and a histone chaperone, FACT. The ssDNA-binding activity of RPA1 was not necessary for this function (Figure 4C), which is consistent with the fact that it is not always correlated with RPA functions (Haring et al., 2008; Hass et al., 2012). As knockdown of RPA1 affected the expression of many genes beyond HSF1 targets (Figure 5A), RPA complex might be involved in chromatin modulation on the whole genome by interacting with other transcription factors.

It was considered unlikely that mammalian HSF1 plays a role in establishing a nucleosome-depleted region of HSP70 promoter, since metazoan HSF1 was thought to bind to DNA only in response to heat shock in vitro and in vivo (Wu, 1984; Larson et al., 1988; Abravaya et al., 1991), and neither human nor *Drosophila* HSF1 alone was unable to bind to the nucleosomal HSP70 promoter in vitro (Becker et al., 1991; Taylor et al., 1991). However, a distinct HSE-binding activity was detected in extracts of non-heat-shocked HeLa cells (Mosser et al., 1988), and metazoan HSF1 bound constitutively to non-HSP genomic loci in vivo (Westwood et al., 1991; Trinklein et al., 2004; Guertin and Lis, 2010). Recent studies revealed that HSF1 opens the chromatin structure of inflammatory genes such as *IL-6* before stimulation (Inouye et al., 2007; Rokavec et al., 2012). Furthermore, it regulated the expression of various proteostasis capacity pathways in unstressed cells (Hayashida et al., 2010, 2011). By identifying a mechanism as described above, we conclude that mammalian HSF1 constitutively gains access to nucleosomal target DNA including HSP70 promoter and suggest it as a "pioneer" transcription factor. As trimer formation of HSF1 was required for its access to nucleosomal DNA (Figure 2F), a small amount of HSF1 trimer could constitutively bind to and activate target genes. This assumption is consistent with the fact that in vivo HSF-binding sites under both heat shock and control conditions are composed of a tandem array of three oppositely oriented NGAAN units in

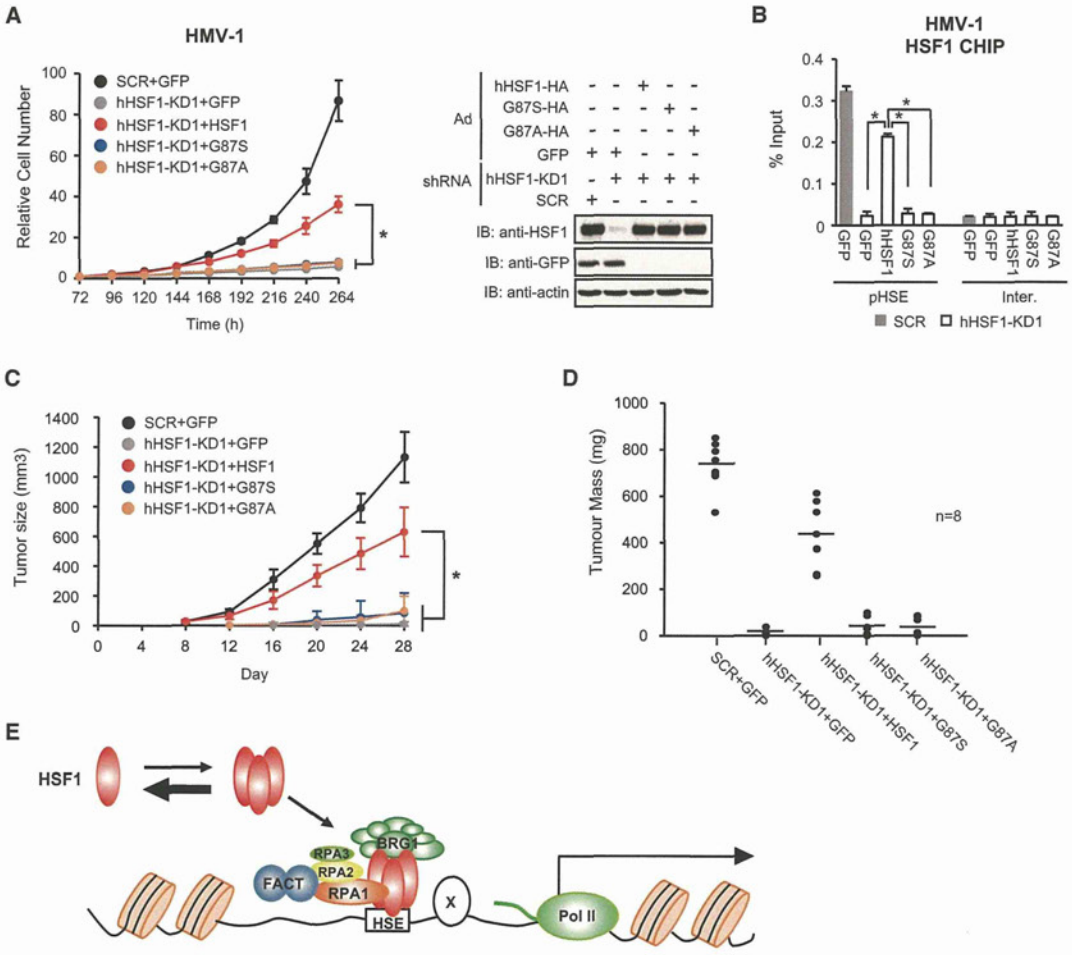

Figure 6. HSF1-RPA Complex Supports Melanoma Cell Proliferation

(A) hHSF1-G87S or hHSF1-G87A was unable to support melanoma cell proliferation in vitro. Endogenous HSF1 was depleted by infection with Ad-sh-hHSF1-KD1 and was replaced with each hHSF1 mutant (hHSF1G87S or G87A) in HMV-1 cells. Relative cell numbers at each time points are shown (left). Error bars, SD (n = 3). Asterisks indicate $p < 0.01$ by ANOVA. Levels of wild-type and mutated hHSF1 at 72 hr were examined by western blotting (right).

(B) HSF1-binding to pHSE of HSP70 promoter. HMV-1 cells were treated as described in (A). ChIP-qPCR analyses on pHSE and intergenic regions were performed using HSF1 antibody at 72 hr. Error bars, SD (n = 3). Asterisks indicate $p < 0.01$ by Student's t test.

(C) Tumor sizes of HMV-1 cells in athymic nude mice. Endogenous HSF1 was depleted by infection with Ad-sh-hHSF1-KD1 and was replaced with each hHSF1 mutant in HMV-1 cells. These cells were injected subcutaneously into athymic nude mice, and sizes of tumors at indicated time points after injection were calculated until 28. Error bars, SD (n = 8). Asterisks indicate $p < 0.01$ by ANOVA.

(D) Tumor mass of HMV-1 cells. Cells were treated as described above, and masses of tumors were determined at 28 days. Bars indicate mean values (n = 8) (see also Figure S7).

(E) Schematic model of chromatin opening by HSF1-RPA complex. Factors cooperatively acting with the complex such as AP-1 and NF-Y are indicated by factor X. BRG1, which is a component of chromatin remodeling complex, binds to the activation domain of HSF1.

Drosophila cells (Guertin and Lis, 2010). Thus, constitutive HSF1 activity, which regulates basal gene expression, might be controlled in part by monomer-to-trimer transition in unstressed cells.

The wing motif of the yeast HSF1 DNA-binding domain does not contact to DNA, nor is it involved in cooperativity between two adjacent HSF1 trimers (Littlefield and Nelson, 1999; Cicero et al., 2001). However, removal of the wing results in a decrease in HSF1-mediated basal transcription in yeast, and substitution of the wing of human HSF1 with that of HSF2 reduces its transcriptional activity, suggesting that the exposed wing might interact with other transcription factors or components of general transcription machinery (Cicero et al., 2001; Ahn et al., 2001). Our finding that the wing of HSF1, but not HSF2, is bound by RPA complex explained the mechanism of its involvement in transcription. Interestingly, HSF1 is dispensable for the proliferation of normal metazoan cells, whereas it is required for that of yeast and human cancer cells (Sorger and Pelham, 1988; Wiederrecht et al., 1988; Dai et al., 2007; Fujimoto and Nakai, 2010). We here demonstrated that HSF1-RPA1 interaction through the

wing, especially glycine at aa 87, is required for the proliferation of cancer cells. This result indicates the involvement of the complex in tumorigenesis and suggests that chemical compounds, which disrupt this interaction by targeting the wing, are attractive candidates for the treatment of cancer patients.

EXPERIMENTAL PROCEDURES

Mass Spectrometry

HEK293 cells were transfected with pShuttle-hHSF1-Flag vector, and the expressed hHSF1-Flag was immunoprecipitated with an anti-Flag antibody. The immunoprecipitates were eluted with a Flag peptide and digested with Lys-C endopeptidase (*Achromobacter* protease I), and the cleaved fragments were directly analyzed by a direct nanoflow liquid chromatography-tandem mass spectrometry (LC-MS/MS) system as previously described (Natsume et al., 2002). Assays were repeated four times.

Coimmunoprecipitation

HEK293 cells transfected with or without expression vectors for HA-tagged mRPAs were lysed with RIPA buffer (25 mM Tris-HCl [pH 7.5], 150 mM NaCl, 1% NP-40, 1% sodium deoxycholate, 0.1% SDS) containing 1 mM PMSF, 1 μg/ml leupeptin, and 1 μg/ml pepstatin. After centrifugation, the supernatant (500 μl) was incubated with 2 μg rabbit polyclonal antibody for HSF1 (αmHSF1j) (Fujimoto et al., 2008) or rat monoclonal antibody for HA (3F10, Roche) at 4°C for 1 hr, and mixed with 20 μl protein A- or protein G-Sepharose beads (GE Healthcare) by rotating at 4°C for 1 hr. The complexes were washed with RIPA buffer and were subjected to western blotting using rabbit antibody for HSF1 (αmHSF1j), mouse monoclonal IgG for HA (Nacalai Tesque, Kyoto, Japan), or goat antibody for SPT16 (C-21, Santa Cruz Biotechnology, Santa Cruz, CA).

RNA Interference

Immortalized MEF cells were infected with an adenovirus expressing each shRNA (1×10^8 pfu/ml) for 2 hr and maintained with normal medium for 70 hr. The cells were treated with heat shock at 42°C for the indicated periods. Knockdown of gene products was confirmed by RT-PCR or western blotting using cell extracts in NP-40 lysis buffer. To knock down the expression of endogenous hRPA1 and overexpress hRPA1 mutants in HeLa cells, the cells were infected with Ad-sh-hRPA1-KD1 (1×10^7 pfu/ml) for 2 hr and maintained with normal medium for 22 hr. They were then infected with adenovirus expressing an hRPA mutant (5×10^6 pfu/ml) for 2 hr and maintained with normal medium for a further 46 hr. Target sequences for knockdown are listed in Table S1.

Assessment of mRNA

Total RNA was isolated from cells using TRIzol (Invitrogen), and first-strand cDNA was synthesized using avian myeloblastosis virus reverse transcriptase (AMV-RT) and oligo $(dT)_{20}$ according to the manufacturer's instructions (Invitrogen). RT-PCR was performed as described previously (Fujimoto et al., 2010) using primers summarized in Table S2. Real-time quantitative PCR (qPCR) was performed using StepOnePlus (Applied Biosystems) with Power SYBR Green PCR master mix (Applied Biosystems) according to the manufacturer's instructions. Primers used for qRT-PCR reactions are listed in Table S3. Relative quantities of mRNAs were normalized against GAPDH mRNA levels. All reactions were performed in triplicate with samples derived from three experiments.

Chromatin Immunoprecipitation Assay

Chromatin immunoprecipitation (ChIP) assay was performed using a kit according to the manufacturer's instructions (EMD Millipore) (Fujimoto et al., 2008), using antibodies for HSF1 (αcHSF1c), RPA1 (sc-28304, Santa Cruz Biotechnology), RPA2 (4E4, Cell Signaling), Pol II (CTD4H8, Millipore), SPT16 (sc-5915, Santa Cruz Biotechnology), Histone H2B (ab1790, Abcam), H3 (ab1791, Abcam), H3K27Ac (ab4729, Abcam), H3K4me3 (ab1012, Abcam), H3K9Ac (07-352, Millipore), SP1 (sc-59, Santa Cruz Biotechnology), and NF-YB (sc-13045, Santa Cruz Biotechnology). Real-time qPCR of the ChIP-enriched DNAs was performed as described above using the primers listed in Table S4. Percentage input was determined by comparing the cycle threshold value of each sample to a standard curve generated from a five-point serial dilution of genomic input. All reactions were performed in triplicate with samples derived from three experiments.

ACCESSION NUMBERS

Microarray data are available in the Gene Expression Omnibus (GEO) database (http://www.ncbi.nlm.nih.gov/geo) through the GEO accession number GSE38412.

SUPPLEMENTAL INFORMATION

Supplemental Information includes seven figures, four tables, and Supplemental Experimental Procedures and can be found with this article online at http://dx.doi.org/10.1016/j.molcel.2012.07.026.

ACKNOWLEDGMENTS

We are grateful to Drs. J. Lis and S. Hirose for valuable comments, and Dr. K. Tanaka for advice on our initial analysis. This work was supported in part by MEXT/JSPS KAKENHI Grant Number 22570171, 24116517, 24390081, Takeda Science Foundation, and the Yamaguchi University Research Project on STRESS.

Received: April 17, 2012
Revised: June 22, 2012
Accepted: July 24, 2012
Published online: August 30, 2012

REFERENCES

Abravaya, K., Phillips, B., and Morimoto, R.I. (1991). Heat shock-induced interactions of heat shock transcription factor and the human hsp70 promoter examined by in vivo footprinting. Mol. Cell. Biol. *11*, 586–592.

Ahn, S.G., Liu, P.C., Klyachko, K., Morimoto, R.I., and Thiele, D.J. (2001). The loop domain of heat shock transcription factor 1 dictates DNA-binding specificity and responses to heat stress. Genes Dev. *15*, 2134–2145.

Akerfelt, M., Morimoto, R.I., and Sistonen, L. (2010). Heat shock factors: integrators of cell stress, development and lifespan. Nat. Rev. Mol. Cell Biol. *11*, 545–555.

Avvakumov, N., Nourani, A., and Côté, J. (2011). Histone chaperones: modulators of chromatin marks. Mol. Cell *41*, 502–514.

Bai, L., Ondracka, A., and Cross, F.R. (2011). Multiple sequence-specific factors generate the nucleosome-depleted region on CLN2 promoter. Mol. Cell *42*, 465–476.

Balch, W.E., Morimoto, R.I., Dillin, A., and Kelly, J.W. (2008). Adapting proteostasis for disease intervention. Science *319*, 916–919.

Becker, P.B., Rabindran, S.K., and Wu, C. (1991). Heat shock-regulated transcription in vitro from a reconstituted chromatin template. Proc. Natl. Acad. Sci. USA *88*, 4109–4113.

Cicero, M.P., Hubl, S.T., Harrison, C.J., Littlefield, O., Hardy, J.A., and Nelson, H.C. (2001). The wing in yeast heat shock transcription factor (HSF) DNA-binding domain is required for full activity. Nucleic Acids Res. *29*, 1715–1723.

Dai, C., Whitesell, L., Rogers, A.B., and Lindquist, S. (2007). Heat shock factor 1 is a powerful multifaceted modifier of carcinogenesis. Cell *130*, 1005–1018.

Duan, Z., Stamatoyannopoulos, G., and Li, Q. (2001). Role of NF-Y in in vivo regulation of the γ-globin gene. Mol. Cell. Biol. *21*, 3083–3095.

Fan, H.Y., He, X., Kingston, R.E., and Narlikar, G.J. (2003). Distinct strategies to make nucleosomal DNA accessible. Mol. Cell *11*, 1311–1322.

Fanning, E., Klimovich, V., and Nager, A.R. (2006). A dynamic model for replication protein A (RPA) function in DNA processing pathways. Nucleic Acids Res. *34*, 4126–4137.

Fuda, N.J., Ardehali, M.B., and Lis, J.T. (2009). Defining mechanisms that regulate RNA polymerase II transcription in vivo. Nature *461*, 186–192.

Fujimoto, M., and Nakai, A. (2010). The heat shock factor family and adaptation to proteotoxic stress. FEBS J. *277*, 4112–4125.

Fujimoto, M., Oshima, K., Shinkawa, T., Wang, B.B., Inouye, S., Hayashida, N., Takii, R., and Nakai, A. (2008). Analysis of HSF4 binding regions reveals its necessity for gene regulation during development and heat shock response in mouse lenses. J. Biol. Chem. *283*, 29961–29970.

Fujimoto, M., Hayashida, N., Katoh, T., Oshima, K., Shinkawa, T., Prakasam, R., Tan, K., Inouye, S., Takii, R., and Nakai, A. (2010). A novel mouse HSF3 has the potential to activate nonclassical heat-shock genes during heat shock. Mol. Biol. Cell *21*, 106–116.

Gajiwala, K.S., and Burley, S.K. (2000). Winged helix proteins. Curr. Opin. Struct. Biol. *10*, 110–116.

Gilmour, D.S., and Lis, J.T. (1985). In vivo interactions of RNA polymerase II with genes of Drosophila melanogaster. Mol. Cell. Biol. *5*, 2009–2018.

Goodwin, A.J., McInerney, J.M., Glander, M.A., Pomerantz, O., and Lowrey, C.H. (2001). In vivo formation of a human β-globin locus control region core element requires binding sites for multiple factors including GATA-1, NF-E2, erythroid Kruppel-like factor, and Sp1. J. Biol. Chem. *276*, 26883–26892.

Green, M., Schuetz, T.J., Sullivan, E.K., and Kingston, R.E. (1995). A heat shock-responsive domain of human HSF1 that regulates transcription activation domain function. Mol. Cell. Biol. *15*, 3354–3362.

Greene, J.M., Larin, Z., Taylor, I.C., Prentice, H., Gwinn, K.A., and Kingston, R.E. (1987). Multiple basal elements of a human hsp70 promoter function differently in human and rodent cell lines. Mol. Cell. Biol. *7*, 3646–3655.

Guertin, M.J., and Lis, J.T. (2010). Chromatin landscape dictates HSF binding to target DNA elements. PLoS Genet. *6*, e1001114.

Guertin, M.J., Martins, A.L., Siepel, A., and Lis, J.T. (2012). Accurate prediction of inducible transcription factor binding intensities in vivo. PLoS Genet. *8*, e1002610.

Haring, S.J., Mason, A.C., Binz, S.K., and Wold, M.S. (2008). Cellular functions of human RPA1. Multiple roles of domains in replication, repair, and checkpoints. J. Biol. Chem. *283*, 19095–19111.

Harrison, C.J., Bohm, A.A., and Nelson, H.C. (1994). Crystal structure of the DNA binding domain of the heat shock transcription factor. Science *263*, 224–227.

Hass, C.S., Lam, K., and Wold, M.S. (2012). Repair-specific functions of replication protein A. J. Biol. Chem. *287*, 3908–3918.

Hayashida, N., Fujimoto, M., Tan, K., Prakasam, R., Shinkawa, T., Li, L., Ichikawa, H., Takii, R., and Nakai, A. (2010). Heat shock factor 1 ameliorates proteotoxicity in cooperation with the transcription factor NFAT. EMBO J. *29*, 3459–3469.

Hayashida, N., Fujimoto, M., and Nakai, A. (2011). Transcription factor cooperativity with heat shock factor 1. Transcription *2*, 91–94.

Inouye, S., Katsuki, K., Izu, H., Fujimoto, M., Sugahara, K., Yamada, S., Shinkai, Y., Oka, Y., Katoh, Y., and Nakai, A. (2003). Activation of heat shock genes is not necessary for protection by heat shock transcription factor 1 against cell death due to a single exposure to high temperatures. Mol. Cell. Biol. *23*, 5882–5895.

Inouye, S., Fujimoto, M., Nakamura, T., Takaki, E., Hayashida, N., Hai, T., and Nakai, A. (2007). Heat shock transcription factor 1 opens chromatin structure of interleukin-6 promoter to facilitate binding of an activator or a repressor. J. Biol. Chem. *282*, 33210–33217.

Kingston, R.E., and Narlikar, G.J. (1999). ATP-dependent remodeling and acetylation as regulators of chromatin fluidity. Genes Dev. *13*, 2339–2352.

Larson, J.S., Schuetz, T.J., and Kingston, R.E. (1988). Activation in vitro of sequence-specific DNA binding by a human regulatory factor. Nature *335*, 372–375.

Le May, N., Mota-Fernandes, D., Vélez-Cruz, R., Iltis, I., Biard, D., and Egly, J.M. (2010). NER factors are recruited to active promoters and facilitate chromatin modification for transcription in the absence of exogenous genotoxic attack. Mol. Cell *38*, 54–66.

Li, G., Levitus, M., Bustamante, C., and Widom, J. (2005). Rapid spontaneous accessibility of nucleosomal DNA. Nat. Struct. Mol. Biol. *12*, 46–53.

Li, B., Carey, M., and Workman, J.L. (2007). The role of chromatin during transcription. Cell *128*, 707–719.

Littlefield, O., and Nelson, H.C. (1999). A new use for the 'wing' of the 'winged' helix-turn-helix motif in the HSF-DNA cocrystal. Nat. Struct. Biol. *6*, 464–470.

Magnani, L., Eeckhoute, J., and Lupien, M. (2011). Pioneer factors: directing transcriptional regulators within the chromatin environment. Trends Genet. *27*, 465–474.

Mavrich, T.N., Jiang, C., Ioshikhes, I.P., Li, X., Venters, B.J., Zanton, S.J., Tomsho, L.P., Qi, J., Glaser, R.L., Schuster, S.C., et al. (2008). Nucleosome organization in the Drosophila genome. Nature *453*, 358–362.

Moldovan, G.L., Pfander, B., and Jentsch, S. (2007). PCNA, the maestro of the replication fork. Cell *129*, 665–679.

Morgan, W.D., Williams, G.T., Morimoto, R.I., Greene, J., Kingston, R.E., and Tjian, R. (1987). Two transcriptional activators, CCAAT-box-binding transcription factor and heat shock transcription factor, interact with a human hsp70 gene promoter. Mol. Cell. Biol. *7*, 1129–1138.

Morimoto, R.I. (2008). Proteotoxic stress and inducible chaperone networks in neurodegenerative disease and aging. Genes Dev. *22*, 1427–1438.

Mosser, D.D., Theodorakis, N.G., and Morimoto, R.I. (1988). Coordinate changes in heat shock element-binding activity and HSP70 gene transcription rates in human cells. Mol. Cell. Biol. *8*, 4736–4744.

Nakamura, Y., Fujimoto, M., Hayashida, N., Takii, R., Nakai, A., and Muto, M. (2010). Silencing HSF1 by short hairpin RNA decreases cell proliferation and enhances sensitivity to hyperthermia in human melanoma cell lines. J. Dermatol. Sci. *60*, 187–192.

Natsume, T., Yamauchi, Y., Nakayama, H., Shinkawa, T., Yanagida, M., Takahashi, N., and Isobe, T. (2002). A direct nanoflow liquid chromatography-tandem mass spectrometry system for interaction proteomics. Anal. Chem. *74*, 4725–4733.

Petesch, S.J., and Lis, J.T. (2008). Rapid, transcription-independent loss of nucleosomes over a large chromatin domain at Hsp70 loci. Cell *134*, 74–84.

Petesch, S.J., and Lis, J.T. (2012). Activator-induced spread of poly(ADP-ribose) polymerase promotes nucleosome loss at Hsp70. Mol. Cell *45*, 64–74.

Richter, K., Haslbeck, M., and Buchner, J. (2010). The heat shock response: life on the verge of death. Mol. Cell *40*, 253–266.

Rokavec, M., Wu, W., and Luo, J.L. (2012). IL6-mediated suppression of miR-200c directs constitutive activation of inflammatory signaling circuit driving transformation and tumorigenesis. Mol. Cell *45*, 777–789.

Saunders, A., Werner, J., Andrulis, E.D., Nakayama, T., Hirose, S., Reinberg, D., and Lis, J.T. (2003). Tracking FACT and the RNA polymerase II elongation complex through chromatin in vivo. Science *301*, 1094–1096.

Schones, D.E., Cui, K., Cuddapah, S., Roh, T.Y., Barski, A., Wang, Z., Wei, G., and Zhao, K. (2008). Dynamic regulation of nucleosome positioning in the human genome. Cell *132*, 887–898.

Sekinger, E.A., Moqtaderi, Z., and Struhl, K. (2005). Intrinsic histone-DNA interactions and low nucleosome density are important for preferential accessibility of promoter regions in yeast. Mol. Cell *18*, 735–748.

Shi, Y., Kroeger, P.E., and Morimoto, R.I. (1995). The carboxyl-terminal transactivation domain of heat shock factor 1 is negatively regulated and stress responsive. Mol. Cell. Biol. *15*, 4309–4318.

Sikorski, T.W., Ficarro, S.B., Holik, J., Kim, T., Rando, O.J., Marto, J.A., and Buratowski, S. (2011). Sub1 and RPA associate with RNA polymerase II at different stages of transcription. Mol. Cell *44*, 397–409.

Smith, S.T., Petruk, S., Sedkov, Y., Cho, E., Tillib, S., Canaani, E., and Mazo, A. (2004). Modulation of heat shock gene expression by the TAC1 chromatin-modifying complex. Nat. Cell Biol. *6*, 162–167.

Sorger, P.K., and Pelham, H.R. (1988). Yeast heat shock factor is an essential DNA-binding protein that exhibits temperature-dependent phosphorylation. Cell *54*, 855–864.

Sullivan, E.K., Weirich, C.S., Guyon, J.R., Sif, S., and Kingston, R.E. (2001). Transcriptional activation domains of human heat shock factor 1 recruit human SWI/SNF. Mol. Cell. Biol. *21*, 5826–5837.

Tang, C.M., Tomkinson, A.E., Lane, W.S., Wold, M.S., and Seto, E. (1996). Replication protein A is a component of a complex that binds the human metallothionein IIA gene transcription start site. J. Biol. Chem. *271*, 21637–21644.

Taylor, I.C., Workman, J.L., Schuetz, T.J., and Kingston, R.E. (1991). Facilitated binding of GAL4 and heat shock factor to nucleosomal templates: differential function of DNA-binding domains. Genes Dev. *5*, 1285–1298.

Trinklein, N.D., Murray, J.I., Hartman, S.J., Botstein, D., and Myers, R.M. (2004). The role of heat shock transcription factor 1 in the genome-wide regulation of the mammalian heat shock response. Mol. Biol. Cell *15*, 1254–1261.

VanDemark, A.P., Blanksma, M., Ferris, E., Heroux, A., Hill, C.P., and Formosa, T. (2006). The structure of the yFACT Pob3-M domain, its interaction with the DNA replication factor RPA, and a potential role in nucleosome deposition. Mol. Cell *22*, 363–374.

Vuister, G.W., Kim, S.J., Orosz, A., Marquardt, J., Wu, C., and Bax, A. (1994). Solution structure of the DNA-binding domain of Drosophila heat shock transcription factor. Nat. Struct. Biol. *1*, 605–614.

Weake, V.M., and Workman, J.L. (2010). Inducible gene expression: diverse regulatory mechanisms. Nat. Rev. Genet. *11*, 426–437.

Westwood, J.T., Clos, J., and Wu, C. (1991). Stress-induced oligomerization and chromosomal relocalization of heat-shock factor. Nature *353*, 822–827.

Wiederrecht, G., Seto, D., and Parker, C.S. (1988). Isolation of the gene encoding the S. cerevisiae heat shock transcription factor. Cell *54*, 841–853.

Wold, M.S. (1997). Replication protein A: a heterotrimeric, single-stranded DNA-binding protein required for eukaryotic DNA metabolism. Annu. Rev. Biochem. *66*, 61–92.

Wu, C. (1984). Activating protein factor binds in vitro to upstream control sequences in heat shock gene chromatin. Nature *311*, 81–84.

Wu, C. (1995). Heat shock transcription factors: structure and regulation. Annu. Rev. Cell Dev. Biol. *11*, 441–469.

Wu, B.J., Kingston, R.E., and Morimoto, R.I. (1986). Human HSP70 promoter contains at least two distinct regulatory domains. Proc. Natl. Acad. Sci. USA *83*, 629–633.

Yuan, G.C., Liu, Y.J., Dion, M.F., Slack, M.D., Wu, L.F., Altschuler, S.J., and Rando, O.J. (2005). Genome-scale identification of nucleosome positions in S. cerevisiae. Science *309*, 626–630.

Zaret, K.S., and Carroll, J.S. (2011). Pioneer transcription factors: establishing competence for gene expression. Genes Dev. *25*, 2227–2241.

Zhang, Y., Moqtaderi, Z., Rattner, B.P., Euskirchen, G., Snyder, M., Kadonaga, J.T., Liu, X.S., and Struhl, K. (2009). Intrinsic histone-DNA interactions are not the major determinant of nucleosome positions in vivo. Nat. Struct. Mol. Biol. *16*, 847–852.

Zobeck, K.L., Buckley, M.S., Zipfel, W.R., and Lis, J.T. (2010). Recruitment timing and dynamics of transcription factors at the Hsp70 loci in living cells. Mol. Cell *40*, 965–975.

Zuo, J., Rungger, D., and Voellmy, R. (1995). Multiple layers of regulation of human heat shock transcription factor 1. Mol. Cell. Biol. *15*, 4319–4330.

FEBS Letters 586 (2012) 3236–3241

FEBS Letters

journal homepage: www.FEBSLetters.org

Acetylation regulates subcellular localization of eukaryotic translation initiation factor 5A (eIF5A)

Muhammad Ishfaq [a,c,d], Kazuhiro Maeta [a], Satoko Maeda [b], Toru Natsume [e], Akihiro Ito [a,b,f,*], Minoru Yoshida [a,b,c,f]

[a] Chemical Genetic Laboratory, RIKEN Advanced Science Institute, 2-1 Hirosawa, Wako, Saitama 351-0198, Japan
[b] Chemical Genomics Research Group, RIKEN Advanced Science Institute, 2-1 Hirosawa, Wako, Saitama 351-0198, Japan
[c] Graduate School of Science and Engineering, Saitama University, 645 Shimo-Okubo, Sakura-ku, Saitama 338-8570, Japan
[d] Department of Biotechnology, Kohat University of Science and Technology, Kohat, Khyber Pakhtunkhwa 26000, Pakistan
[e] Biomedicinal Information Research Center, The National Institute of Advanced Industrial Science and Technology, Aomi 2-4-7, Koto-ku, Tokyo 135-0064, Japan
[f] Japan Science and Technology Corporation, CREST Research Project, Kawaguchi, Saitama 332-0012, Japan

ARTICLE INFO

Article history:
Received 23 May 2012
Revised 22 June 2012
Accepted 22 June 2012
Available online 4 July 2012

Edited by Michael Ibba

Keywords:
eIF5A
Acetylation
Hypusination
Subcellular localization

ABSTRACT

Eukaryotic translation initiation factor 5A (eIF5A) is a protein subject to hypusination, which is essential for its function. eIF5A is also acetylated, but the role of that modification is unknown. Here, we report that acetylation regulates the subcellular localization of eIF5A. We identified PCAF as the major cellular acetyltransferase of eIF5A, and HDAC6 and SIRT2 as its major deacetylases. Inhibition of the deacetylases or impaired hypusination increased acetylation of eIF5A, leading to nuclear accumulation. As eIF5A is constitutively hypusinated under physiological conditions, we suggest that reversible acetylation plays a major role in controlling the subcellular localization of eIF5A.

1. Introduction

eIF5A is a small (~17 KDa) acidic protein that is essential for cell proliferation in many eukaryotes. Mammals have two paralogs, eIF5A1 and eIF5A2. eIF5A1 is ubiquitously expressed in all tissues [1–3] and is modified post-translationally with an unusual amino acid, hypusine [Ne-(4-amino-2-hydroxybutyl)lysine] [4]. Hypusine is synthesized from the polyamine spermidine in two consecutive enzymatic steps: first, deoxyhypusine synthase (DHS) catalyzes the transfer of the aminobutyl moiety from spermidine to a specific lysine residue (Lys50 in human eIF5A) to form the deoxyhypusine intermediate, which is ultimately hydroxylated by deoxyhypusine hydroxylase (DOHH) to produce active hypusinated eIF5A [5]. eIF5A and its hypusine modification are essential in cellular physiology: hypusination mutants exhibit slowed cell growth in mammals [6]; in yeast, a hypusination site mutant (K51R) fails to rescue the eIF5A knockout [3]. Although eIF5A is evidently essential for eukaryotic cell proliferation [2,7,8], its precise function has remained unknown. eIF5A was originally identified, along with other initiation factors, from high-salt washes of rabbit reticulocytes lysate ribosomes [9], and was shown to stimulate methionyl-puromycin synthesis [10]; therefore, eIF5A was considered to be a translational initiation factor. However, recent findings suggest that it plays a role in translation elongation [11] and other aspects of RNA metabolism such as RNA export [12,13].

The subcellular localization of eIF5A and its involvement in nuclear export have remained controversial. eIF5A was initially demonstrated to be localized at the nuclear pore complex, where it is involved in Rev-mediated nuclear export of unspliced HIV-1 mRNAs [12]. However, Shi et al. showed that eIF5A is cytoplasmic in a variety of cell types, and that HIV-1 Rev overexpression does not affect its cellular distribution [14]. Subsequently, Rosorius et al. demonstrated that eIF5A undergoes nucleo-cytoplasmic shuttling, and proposed that CRM1 acts as its nuclear export factor [15]. Although eIF5A lacks a conventional nuclear import signal, experiments with GFP-tagged truncated eIF5A suggested that the ~19 N-terminal residues are responsible for eIF5A nuclear localization [16]. eIF5A regulates diverse cellular processes, including induction of p53-dependent apoptosis and cytokine-mediated islet β cell

* Corresponding author at: Chemical Genetic Laboratory, RIKEN Advanced Science Institute, 2-1 Hirosawa, Wako, Saitama 351-0198, Japan. Fax: +81 48 462 4676.
E-mail address: akihiro-i@riken.jp (A. Ito).

0014-5793/$36.00
http://dx.doi.org/10.1016/j.febslet.2012.06.042

dysfunction [17,18], suggesting a functional role for eIF5A in the nucleus. Recently, Lee et al. demonstrated that exogenously produced eIF5A is primarily expressed as an unhypusinated precursor, and can only be hypusinated when co-expressed with DHS and DOHH. Moreover, unhypusinated GFP-eIF5A is primarily localized in the nucleus, whereas the hypusinated form is cytoplasmic, suggesting that hypusination determines the subcellular distribution of eIF5A [19]. However, because hypusination occurs on almost all eIF5A proteins, co-translationally [20] and irreversibly, hypusination seems unlikely to be responsible for the dynamic regulation of nucleo-cytoplasmic transport under physiological conditions. eIF5A residues K47 and K68 are post-translationally modified by acetylation [20,21]. The crystal structure of human eIF5A consists of two domains of predominantly β-sheet character [22]. The acetylation and hypusination sites (i.e. K47 and K50, respectively) are in close proximity on a disordered loop structure, the hypusine loop, in the N-terminal domain. The positive charge at K47 is essential for eIF5A activity, suggesting that acetylation at this position negatively regulates eIF5A function in protein synthesis [23]. However, the role of eIF5A acetylation in other functions remains elusive.

In this study, we found that the acetylated form of eIF5A is primarily enriched in the nucleus, whereas unacetylated eIF5A is primarily cytoplasmic; this distinction is even more pronounced in the presence of histone deacetylase (HDAC) inhibitors. These results suggest that acetylation acts as a molecular switch for eIF5A, allowing it to exert distinct functions in the cytoplasm and nucleus.

2. Materials and methods

2.1. Compounds, cell culture and transfection

Tricostatin A (TSA) and nicotinamide (NA) were purchased from Wako Chemicals. GC7 was purchased from BIOSEARCH TECHNOLOGIES, INC., SCOP402 was kindly provided by Dr. Norikazu Nishino (Kyushu Institute of Technology, Japan). All compounds were prepared as stock solutions in dimethyl sulfoxide (DMSO) and stored at −20 °C. 293T and HeLa cells were transiently transfected with expression vectors using the FuGENE® HD reagent (Roche) and the Lipofectamine™ LTX reagent (Invitrogen), respectively. RNAi oligos used in this study were obtained from Dharmacon, with the exception of the eIF5A and HDAC1 oligos, which were obtained from Nippon Gene. All sequence information of siRNA oligos is described in Supplemental Table 1.

2.2. Plasmids construction

The cDNA encoding human eIF5A was PCR-amplified from a human brain cDNA library and sub-cloned into either GFP-pEGFP (BD Biosciences) or to the C-terminus of Flag-tag in pcDNA3 (Invitrogen). Plasmids for expression of GFP-eIF5A and Flag-eIF5A mutant proteins (K47R, K47Q, K50R, and K47,50R) were generated by site-directed mutagenesis using primer sets containing the desired mutations. DNA encoding human DHS was PCR-amplified from a human brain cDNA library and sub-cloned into pcDNA3-Flag. The pcEFL-DOHH construct was kindly provided by Dr. Myung Hee Park (National Institute of Health, USA); the coding sequence was PCR-amplified and sub-cloned into the pcDNA3-Myc vector.

2.3. Antibodies and immunoblotting

A rabbit polyclonal antibody against acetylated eIF5A was raised using an acetylated eIF5A peptide (VDMSTSK(Ac)TGKHGHC) with the aid of the Support Unit for Bio-material Analysis and Animal Resources Development at the RIKEN BSI Research Resources Center (RRC). A mouse monoclonal antibody against hypusinated eIF5A was raised using a hypusinated eIF5A peptide (STSKTGK(Hyp)HGHAKC). Mouse monoclonal anti-Flag M2, anti-α-tubulin (B-5-1-2), and anti-Ac-α-tubulin (6-11B-1) antibodies were purchased from Sigma. Monoclonal anti-c-Myc (9E10) and monoclonal anti-eIF5A antibodies were obtained from Santa Cruz Biotechnology and BD Bioscience, respectively. Rabbit polyclonal anti-CBP, anti-PCAF, anti-GCN5, anti-SIRT1, and anti-SIRT2 antibodies were purchased from Cell Signaling Technology. Immunoblotting was performed using whole cell lysates, prepared by collecting washed cells directly in 1× SDS–PAGE sample loading buffer and heating at 95 °C for 5 min. Equal volumes of each whole cell lysate was resolved by SDS–PAGE and transferred to a polyvinylidene difluoride membrane (Millipore) by electroblottting. Membranes were incubated with primary and secondary antibodies; immune complexes were detected using the Immobilon™ Western Chemiluminescent HRP substrate (Millipore); and luminescence was analyzed using a LAS-3000 image analyzer (GE Healthcare).

2.4. Immunostaining and fluorescence microscopy

Cells grown on coverslips were fixed in 4% paraformaldehyde for 15 min and permeabilized in 0.2% Triton X-100 in PBS (PBT). Fixed cells were blocked with 5% normal goat serum in 0.1% PBT for 15 min and incubated with primary antibodies against eIF5A (1:200 dilution), Ac-eIF5A (1:100), Flag (1:500), or Myc (1:500) for 1–2 h followed by the Alexa Fluor 594, Alexa Fluor 488, or Alexa Fluor 350 secondary antibodies (Invitrogen) for 20 min. Slides were mounted with mounting medium (Vector Laboratories), and images were taken using a Delta Vision Microscope (SEKI Technotron Corp.).

2.5. In vitro histone acetyltransferases (HATs) assay

Recombinant His-tagged eIF5A was purified as described previously [24]. In vitro HAT assays were performed as described previously [24] with minor modifications: briefly, 8 μg of His-eIF5A was incubated with 8.5 μg of purified Flag-PCAF in the presence of 0.33 mM acetyl CoA. The reaction was performed at 37 °C for 1 h. The samples were mixed with reducing/loading buffer and resolved by SDS–PAGE on 13% polyacrylamide gels followed by immunoblotting with the indicated antibodies.

3. Results and discussion

3.1. Hypusination inhibits acetylation

Using an anti-acetylated lysine (Ac-Lys) antibody and radioactively labeled spermidine, Lee et al. observed that co-transfection with DHS and DOHH enables hypusination of eIF5A exogenously expressed in mammalian cells; furthermore, unhypusinated eIF5A expressed in the absence of DHS and DOHH is heavily acetylated at K47 but is dramatically deacetylated upon hypusination, suggesting crosstalk between hypusination and acetylation [19]. We first confirmed these observations using a newly developed anti-acetylated eIF5A (Ac-eIF5A), and an anti-hypusinated eIF5A (Hyp-eIF5A) antibody. Exogenously expressed eIF5A could be hypusinated only when co-expressed with DHS and DOHH (Fig. 1A). In addition, DHS and DOHH expression reduced the acetylation at K47 (Fig. 1A). The specificity of the antibodies was confirmed by detecting acetylation and hypusination of K47R and K50R mutants as well as wild-type eIF5A overexpressed in 293T cells with or without DHS/DOHH (Fig. 1B). In the absence of DHS and DOHH, wild-type Flag-eIF5A was heavily acetylated, but the acetylation signal was completely lost in K47R, indicating that the antibody can specifically recognize eIF5A acetylated at K47. The hypusination signal

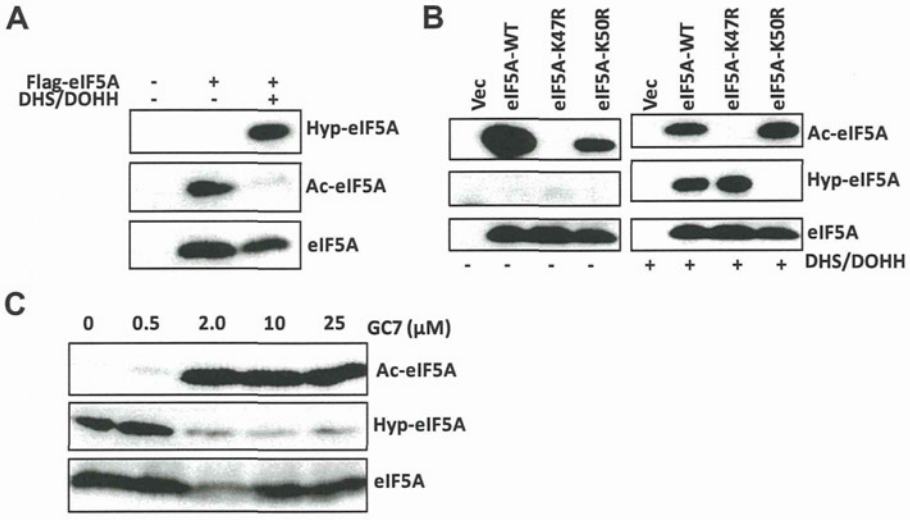

Fig. 1. Interplay between eIF5A acetylation and hypusination. (A, B) 293T cells were transfected with FLAG-eIF5A wild-type (WT), acetylation site (K47R), or hypusination site (K50R) mutants in the presence or absence of pcDNA3-hDHS and pcDNA3-hDOHH. Whole-cell lysates were immunoblotted with the indicated antibodies. The blots show exogenously expressed eIF5A. (C) Whole-cell lysates from HeLa cells treated for 16 h with different concentrations of the DHS inhibitor GC7 were immunoblotted with the indicated antibodies.

was detected in exogenously expressed eIF5A proteins in the presence of DHS and DOHH, but not in the K50R mutant lacking the hypusination site. Hypusination of the K47R mutant, which is defective in acetylation, suggests that acetylation is not required hypusination. To further observe the relationship between hypusination and acetylation, we treated HeLa cells with different concentrations of GC7, a DHS inhibitor, for 16 h. Immunoblot analysis showed that GC7 inhibited eIF5A hypusination at a concentration as low as 2 μM. While the eIF5A acetylation level was low in cells treated with GC7 at a low concentration (0.5 μM), it was dramatically increased by 2 μM or higher concentrations, confirming that hypusination negatively regulates acetylation (Fig. 1C). Endogenous eIF5A in the steady state is poorly acetylated because eIF5A is fully hypusinated in the absence of GC7 (Fig. 1C). Because crystal structure analysis revealed that the two lysine residues for acetylation and hypusination are closed [22], hypusination may hinder the access of the eIF5A acetyltransferase, PCAF (see below).

3.2. Identification of HATs and HDACs regulating eIF5A acetylation status

To identify the cellular acetyltransferase responsible for eIF5A acetylation, we next performed siRNA-mediated knockdown experiments using 293T cells (Fig. 2A). Of four acetyltransferases tested, only PCAF knockdown significantly reduced the acetylation level of endogenous eIF5A. Furthermore, in an in vitro HAT assay using bacterially produced recombinant eIF5A, we found that PCAF indeed acetylates eIF5A in an acetyl-CoA-dependent manner (Fig. 2B). To identify the class of HDACs involved in deacetylation of eIF5A, we treated 293T cells with three HDAC inhibitors of differing specificity: TSA, NA, and SCOP402. TSA inhibits all class I/II enzymes, whereas NA inhibits class III; SCOP402 inhibits class I/II enzymes except HDAC6 [25]. Immunoblot analysis of the cell lysates collected after 16 h incubation with the HDAC inhibitors showed that acetylated eIF5A was increased in both TSA- and NA-treated cells but not in SCOP402-treated cells (Fig. 2C). Because the only difference in target enzyme specificity between TSA and SCOP401 is HDAC6 inhibition, we conclude that at least HDAC6 is involved in deacetylation of eIF5A. The acetylation signal was significantly enhanced in cells treated with both TSA and NA simultaneously, suggesting that a class III HDAC in addition to HDAC6 is also involved in the eIF5A deacetylation. Importantly, the level of eIF5A hypusination was not changed in response to treatment with HDAC inhibitors (Fig. 2C), suggesting that acetylation does not affect its hypusination. Next, we expressed ten major cellular deacetylase enzymes together with Flag-eIF5A in 293T cells (Fig. 2D, S1A). Only overexpression of HDAC6 or SIRT2, but not their catalytically dead mutants, significantly reduced the acetylation level of eIF5A. Consistent with this, the acetylation level of endogenous eIF5A was greatly increased by HDAC6 and SIRT2 knockdown in 293T cells (Fig. 2E), indicating that these enzymes actually work as deacetylases under physiological conditions. Additionally, SIRT1 overexpression slightly but reproducibly reduced eIF5A acetylation. Indeed, both recombinant SIRT1 and SIRT2 catalyzed the deacetylation of eIF5A in an in vitro deacetylase assay (Fig. S1B–C). However, the SIRT1 knockdown failed to increase endogenous eIF5A acetylation in 293T cells (Fig. 2E). These results indicate that HDAC6 and SIRT2 are the major cellular deacetylases of eIF5A.

3.3. Effect of acetylation and hypusination on subcellular distribution of eIF5A

Lee et al. reported that hypusination is important for the localization of eIF5A to the cytoplasm, where translation occurs [19]. In general, reversible acetylation plays a role in regulating protein–protein interactions and subcellular localization. As the acetylation site is located within a loop close to the hypusination site (K50), it seemed possible that eIF5A acetylation plays some role in the subcellular localization of eIF5A. Therefore, we investigated the subcellular localization of acetylated species of endogenous eIF5A by indirect immunofluorescence. Although total eIF5A was primarily cytoplasmic in nature, acetylated eIF5A was predominately localized to the nucleus (Fig. 3A). The fluorescent signals obtained with eIF5A and Ac-eIF5A antibodies are specific, because these signals were diminished, respectively, by eIF5A knockdown and by competition with the acetylated peptide used as the epitope (Fig. 3A). Furthermore, treatment with either HDAC inhibitors (TSA/NA) or DHS inhibitor (GC7) induced a dramatic shift of subcellular distribution from primarily cytoplasmic to nuclear (Fig. 3B). These results clearly demonstrate that cytoplasmic eIF5A is not

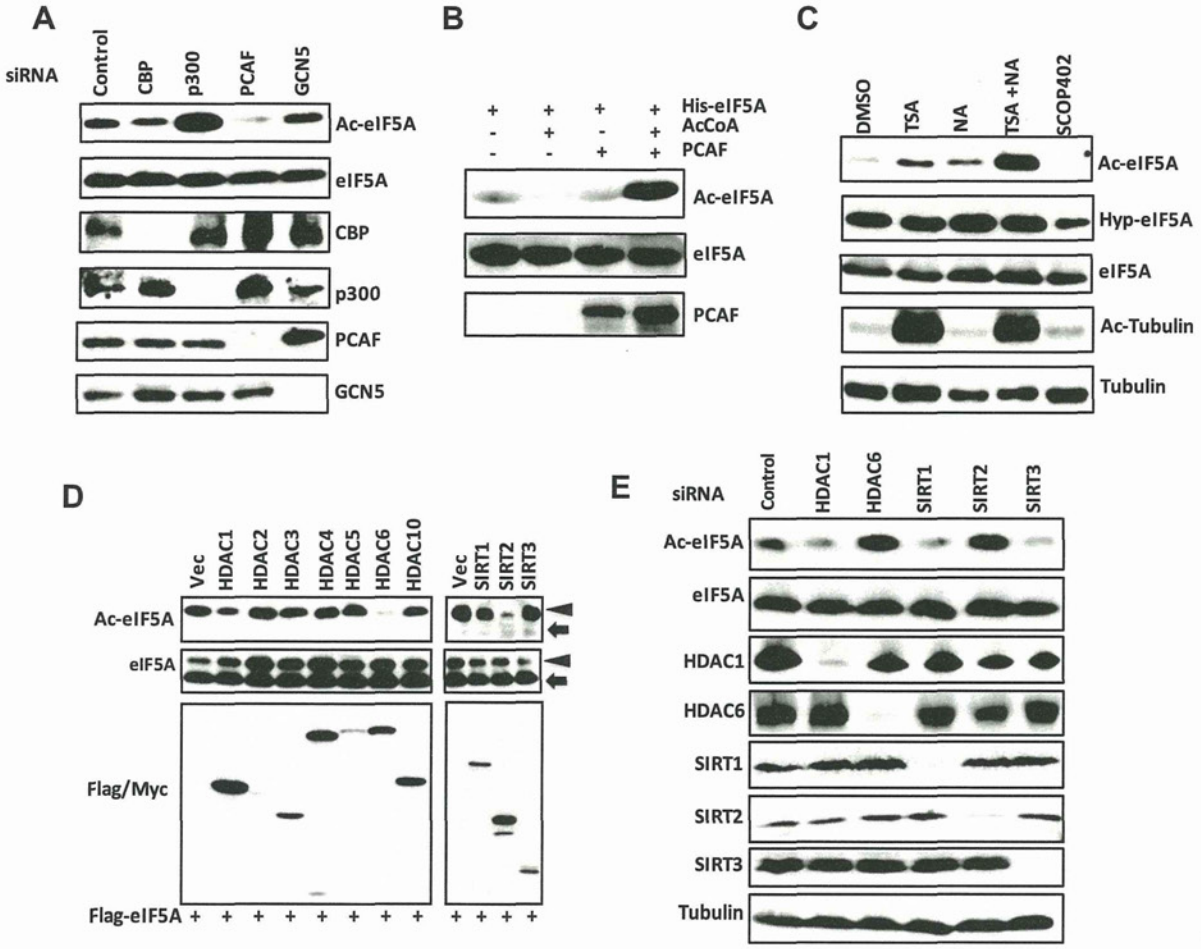

Fig. 2. Identification of the acetyltransferases (HATs) and deacetylases (HDACs) of eIF5A. (A) Effects of siRNA mediated-knockdown of different HATs on eIF5A acetylation in 293T cells. 293T cells were transfected with siRNA oligos against the indicated HATs for 72 h, and whole-cell lysates were immunoblotted with the indicated antibodies. (B) In vitro acetylation of eIF5A by recombinant PCAF. Recombinant His-tagged eIF5A was incubated with recombinant PCAF in the presence or absence of acetyl-CoA; the reaction mixture was immunoblotted with the indicated antibodies. (C) Effects of HDAC inhibitors on eIF5A acetylation. Whole-cell lysates from 293T cells treated with TSA, NA, a mixture of TSA and NA, or SCOP402 were immunoblotted with the indicated antibodies. (D) Effects of overexpression of HDACs on eIF5A acetylation. Whole-cell lysates from 293T cells overexpressing the indicated flag tagged class I/II HDACs or myc tagged class III HDACs were immunoblotted with the indicated antibodies including the mixture of anti-flag and anti-myc antibodies (Flag/Myc). An arrowhead and a block arrow indicate exogenous and endogenous eIF5A, respectively (E) Effects of siRNA-mediated knockdown of different HDACs on eIF5A acetylation in 293T cells. 293T cells were transfected with siRNA oligos against the indicated HDACs for 72 h; whole-cell lysates were immunoblotted with the indicated antibodies.

acetylated, whereas nuclear eIF5A is acetylated; furthermore, acetylation directs nuclear localization.

Next we tested whether eIF5A K47 acetylation is indeed important for controlling the subcellular localization of eIF5A, by expressing GFP-eIF5A and its mutants. As shown in Fig. 4A, unhypusinated GFP-eIF5A expressed in the absence of DHS/DOHH tended to localize to the nucleus. On the other hand, both wild-type eIF5A and a mutant incapable of being acetylated (K47R) were successfully localized to the cytoplasm when hypusinated by DHS/DOHH (Fig. 4A). Importantly, the subcellular distribution of a mutant mimicking acetylation (K47Q) was constitutively nuclear even after hypusination by DHS/DOHH (Fig. 4A–B), suggesting that acetylation interferes with the eIF5A nuclear export. Similarly, the K50R mutant, which is unhypusinated but heavily acetylated, also accumulated in the nucleus. The K47,50R mutant, which can be neither acetylated nor hypusinated, was also localized to the nucleus (Fig. 4A–B). These results indicate that cytoplasmic localization of eIF5A requires not only hypusination but also hypoacetylation.

Various groups studying the subcellular localization of eIF5A have reported somewhat inconsistent results. For instance, Xiao et al. reported that eIF5A is cytoplasmic and co-localizes with the endoplasmic reticulum in multiple mammalian cell lines [26]. In contrast, Rosorius et al. proposed that eIF5A undergoes nucleo-cytoplasmic shuttling and co-localizes with the nuclear pore complex; these authors identified CRM1 as the corresponding nuclear export factor [15]. Jao et al. also suggested that eIF5A enters the nucleus through passive diffusion and may be exported from the nucleus in a CRM1-dependent manner [27]. On the other hand, other groups showed that exportin 4, an importin β family receptor, is responsible for the nuclear export of eIF5A [13,28]. Recently Lee et al. reported that compared to fully hypusinated cytoplasmic, endogenous eIF5A, exogenously expressed eIF5A lacking hypusination tends to localize in the nucleus, but can be relocalized to the cytoplasm when fully hypusinated [19]. Compared to the stable hypusine modification, acetylation is reversible and may play an important role in regulating eIF5A cellular activity by altering the conformation of the hypusine loop or eIF5A's affinity for nuclear transport factors. Thus, control of subcellular localization of eIF5A appears to be dependent more on acetylation than on hypusination under the physiological condition. Our data indicate that co-translationally hypusinated eIF5A is acetylated by PCAF and deacetylated by HDAC6 and SIRT2, which facilitates nucleo-cytoplasmic

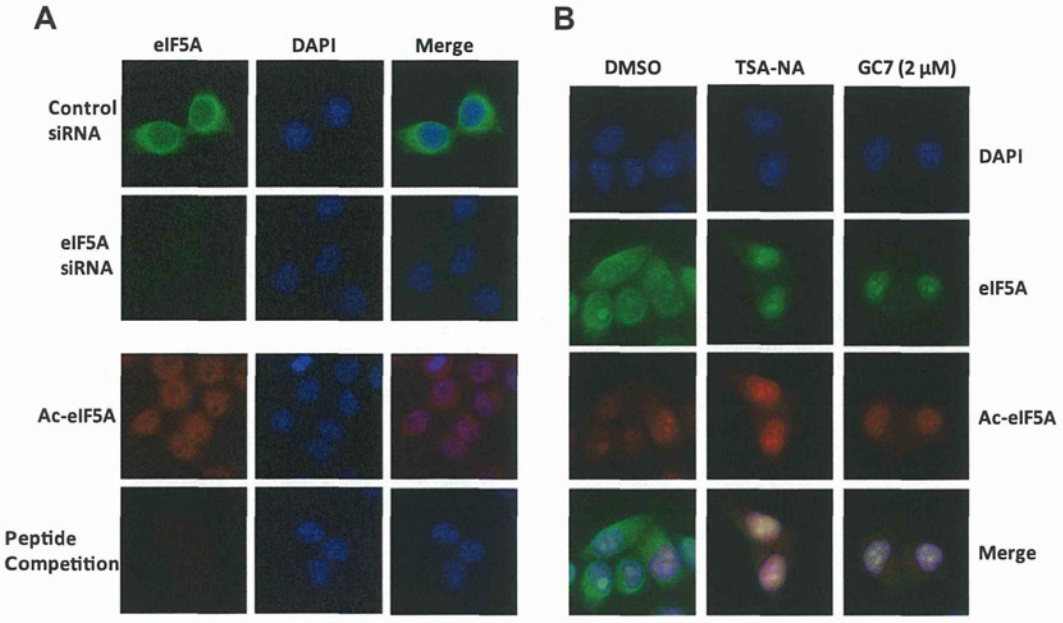

Fig. 3. Subcellular distribution of endogenous acetylated eIF5A. (A) HeLa cells treated with either control (upper panels) or eIF5A (lower panels) siRNA oligo were immunostained with anti-eIF5A antibody. Subcellular distribution of acetylated eIF5A was determined by immunostaining with anti-Ac-eIF5A antibody (upper panels); specificity of the antibody was determined using competition with Ac-eIF5A peptide (lower panels). (B) Subcellular distributions of total and acetylated eIF5A in HeLa cells treated with DMSO, TSA and NA, or GC7 were determined by immunoblotting with anti-eIF5A and anti-Ac-eIF5A antibodies.

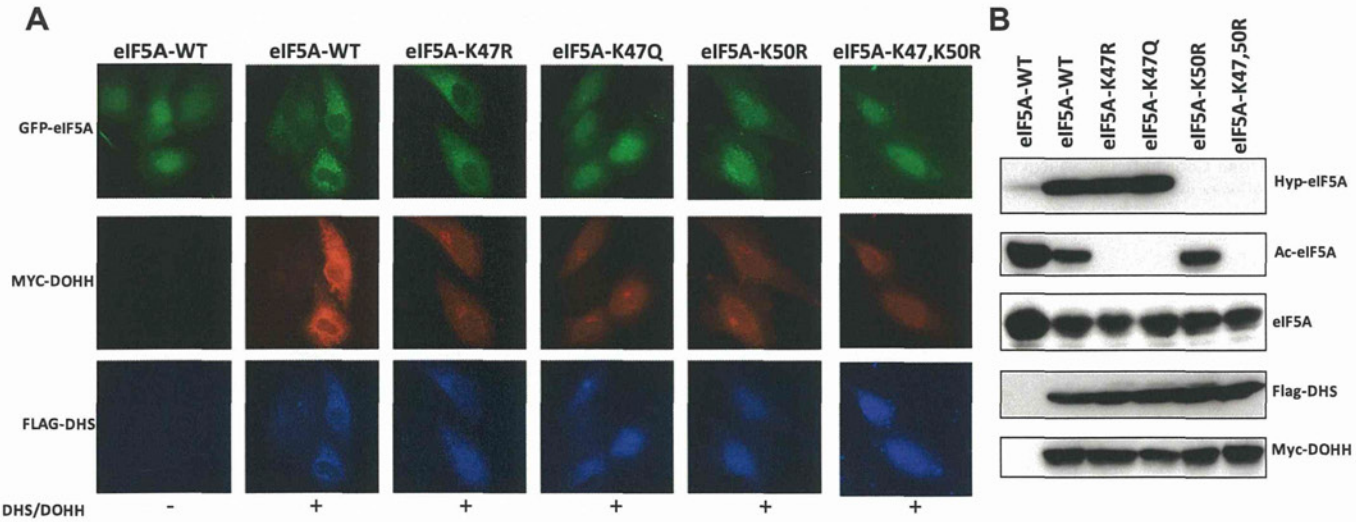

Fig. 4. Subcellular distributions of acetylation and hypusination mutants of GFP-fused eIF5A. (A) HeLa cells were transfected with the indicated GFP-eIF5A constructs in the presence or absence of myc-hDOHH and Flag-hDHS; and immunostained with anti-myc and anti-FLAG antibodies in order to detect hDOHH and hDHS, respectively. (B) Acetylation and hypusination status of modification-site mutants of eIF5A. Whole-cell lysates of HeLa cells overexpressing the indicated GFP-fused eIF5A constructs with or without hDHS and hDOHH were immunoblotted with the indicated antibodies.

shuttling of eIF5A. Although the nuclear function of eIF5A is still unclear, the evolutionarily conserved acetylation occurring near the site of hypusination may regulate its nuclear localization and its function in the nucleus.

4. Conclusion

We have elucidated the enzymes responsible for determining the acetylation status of eIF5A K47: PCAF performs acetylation, while HDAC6 and SIRT2 perform deacetylation. Our results suggest that eIF5A acetylation status regulates its subcellular localization. This knowledge will enable us to study the possible functional role of this important protein in the nuclear compartment under physiological conditions.

Acknowledgments

We thank Dr. Myung Hee Park and Dr. Norikazu Nishino, respectively, for the kind gifts of the hDHS construct and SCOP402. This work was supported in part by the Chemical Genomics Research Project; RIKEN ASI; the CREST Research Project; the Japan Science and Technology Corporation; and a Grant-in-Aid for Scientific Research on Priority Area "Cancer" from the Ministry of Education, Culture, Sports, Science and Technology of Japan.

Appendix A. Supplementary data

Supplementary data associated with this article can be found, in the online version, at http://dx.doi.org/10.1016/j.febslet.2012.06.042.

References and notes

[1] Chen, K.Y. and Liu, A.Y. (1997) Biochemistry and function of hypusine formation on eukaryotic initiation factor 5A. Biol. Signals 6, 105–109.

[2] Park, M.H., Lee, Y.B. and Joe, Y.A. (1997) Hypusine is essential for eukaryotic cell proliferation. Biol. Signals 6, 115–123.

[3] Schnier, J., Schwelberger, H.G., Smit-McBride, Z., Kang, H.A. and Hershey, J.W. (1991) Translation initiation factor 5A and its hypusine modification are essential for cell viability in the yeast Saccharomyces cerevisiae. Mol. Cell. Biol. 11, 3105–3114.

[4] Cooper, H.L., Park, M.H., Folk, J.E., Safer, B. and Braverman, R. (1983) Identification of the hypusine-containing protein hy+ as translation initiation factor eIF-4D. Proc. Natl. Acad. Sci. U S A 80, 1854–1857.

[5] Park, M.H. (2006) The post-translational synthesis of a polyamine-derived amino acid, hypusine, in the eukaryotic translation initiation factor 5A (eIF5A). J. Biochem. 139, 161–169.

[6] Park, M.H., Wolff, E.C. and Folk, J.E. (1993) Is hypusine essential for eukaryotic cell proliferation? Trends Biochem. Sci. 18, 475–479.

[7] Park, M.H., Wolff, E.C., Lee, Y.B. and Folk, J.E. (1994) Antiproliferative effects of inhibitors of deoxyhypusine synthase. Inhibition of growth of Chinese hamster ovary cells by guanyl diamines. J. Biol. Chem. 269, 27827–27832.

[8] Hanauske-Abel, H.M., Park, M.H., Hanauske, A.R., Popowicz, A.M., Lalande, M. and Folk, J.E. (1994) Inhibition of the G1-S transition of the cell cycle by inhibitors of deoxyhypusine hydroxylation. Biochim. Biophys. Acta 1221, 115–124.

[9] Benne, R. and Hershey, J.W. (1978) The mechanism of action of protein synthesis initiation factors from rabbit reticulocytes. J. Biol. Chem. 253, 3078–3087.

[10] Park, M.H. (1989) The essential role of hypusine in eukaryotic translation initiation factor 4D (eIF-4D). Purification of eIF-4D and its precursors and comparison of their activities. J. Biol. Chem. 264, 18531–18535.

[11] Saini, P., Eyler, D.E., Green, R. and Dever, T.E. (2009) Hypusine-containing protein eIF5A promotes translation elongation. Nature 459, 118–121.

[12] Ruhl, M. et al. (1993) Eukaryotic initiation factor-5a is a cellular target of the human-immunodeficiency-virus type-1 rev activation domain mediating transactivation. J. Cell Biol. 123, 1309–1320.

[13] Lipowsky, G., Bischoff, F.R., Schwarzmaier, P., Kraft, R., Kostka, S., Hartmann, E., Kutay, U. and Gorlich, D. (2000) Exportin 4: a mediator of a novel nuclear export pathway in higher eukaryotes. EMBO J. 19, 4362–4371.

[14] Yang, X.J., Ogryzko, V.V., Nishikawa, J., Howard, B.H. and Nakatani, Y. (1996) A p300/CBP-associated factor that competes with the adenoviral oncoprotein E1A. Nature 382, 319–324.

[15] Rosorius, O., Reichart, B., Kratzer, F., Heger, P., Dabauvalle, M.C. and Hauber, J. (1999) Nuclear pore localization and nucleocytoplasmic transport of eIF-5A: evidence for direct interaction with the export receptor CRM1. J. Cell Sci. 112 (Pt 14), 2369–2380.

[16] Parreiras, E.S.L.T., Gomes, M.D., Oliveira, E.B. and Costa-Neto, C.M. (2007) The N-terminal region of eukaryotic translation initiation factor 5A signals to nuclear localization of the protein. Biochem. Biophys. Res. Commun. 362, 393–398.

[17] Li, A.L. et al. (2004) A novel eIF5A complex functions as a regulator of p53 and p53-dependent apoptosis. J. Biol. Chem. 279, 49251–49258.

[18] Maier, B. et al. (2010) The unique hypusine modification of eIF5A promotes islet beta cell inflammation and dysfunction in mice. J. Clin. Invest. 120, 2156–2170.

[19] Lee, S.B., Park, J.H., Kaevel, J., Sramkova, M., Weigert, R. and Park, M.H. (2009) The effect of hypusine modification on the intracellular localization of eIF5A. Biochem. Biophys. Res. Commun. 383, 497–502.

[20] Park, M.H. (1988) The identification of an eukaryotic initiation factor 4D precursor in spermidine-depleted Chinese hamster ovary cells. J. Biol. Chem. 263, 7447–7449.

[21] Klier, H., Csonga, R., Joao, H.C., Eckerskorn, C., Auer, M., Lottspeich, F. and Eder, J. (1995) Isolation and structural characterization of different isoforms of the hypusine-containing protein eIF-5A from HeLa cells. Biochemistry 34, 14693–14702.

[22] Tong, Y.F., Park, I., Hong, B.S., Nedyalkova, L., Tempel, W. and Park, H.W. (2009) Crystal structure of human eIF5A1: Insight into functional similarity of human eIF5A1 and eIF5A2. Proteins 75, 1040–1045.

[23] Dias, C.A. et al. (2008) Structural modeling and mutational analysis of yeast eukaryotic translation initiation factor 5A reveal new critical residues and reinforce its involvement in protein synthesis. FEBS J. 275, 1874–1888.

[24] Fukuda, I. et al. (2009) Ginkgolic acid inhibits protein SUMOylation by blocking formation of the E1-SUMO intermediate. Chem. Biol. 16, 133–140.

[25] Nishino, N., Jose, B., Okamura, S., Ebisusaki, S., Kato, T., Sumida, Y. and Yoshida, M. (2003) Cyclic tetrapeptides bearing a sulfhydryl group potently inhibit histone deacetylases. Org. Lett. 5, 5079–5082.

[26] Shi, X.P., Yin, K.C., Zimolo, Z.A., Stern, A.M. and Waxman, L. (1996) The subcellular distribution of eukaryotic translation initiation factor, eIF-5A, in cultured cells. Exp. Cell Res. 225, 348–356.

[27] Jao, D.L. and Yu Chen, K. (2002) Subcellular localization of the hypusine-containing eukaryotic initiation factor 5A by immunofluorescent staining and green fluorescent protein tagging. J. Cell. Biochem. 86, 590–600.

[28] Zender, L. et al. (2008) An oncogenomics-based in vivo RNAi screen identifies tumor suppressors in liver cancer. J. Cell Biol. 135, 852–864.

Biochemical and Biophysical Research Communications 423 (2012) 122–127

Contents lists available at SciVerse ScienceDirect

Biochemical and Biophysical Research Communications

journal homepage: www.elsevier.com/locate/ybbrc

Insulin/insulin-like growth factor (IGF) stimulation abrogates an association between a deubiquitinating enzyme USP7 and insulin receptor substrates (IRSs) followed by proteasomal degradation of IRSs

Hidehito Yoshihara [a], Toshiaki Fukushima [a,b], Fumihiko Hakuno [a], Yasushi Saeki [c], Keiji Tanaka [c], Akihiro Ito [d], Minoru Yoshida [d], Shun-ichiro Iemura [e], Tohru Natsume [e], Tomoichiro Asano [b], Kazuhiro Chida [a], Leonard Girnita [f], Shin-Ichiro Takahashi [a,*]

[a] Department of Animal Sciences and Applied Biological Chemistry, Graduate School of Agriculture and Life Sciences, The University of Tokyo, Tokyo, Japan
[b] Laboratory of Biomedical Chemistry, Institute of Biomedical and Health Sciences, Hiroshima University, Hiroshima, Japan
[c] Laboratory of Protein Metabolism, Tokyo Metropolitan Institute of Medical Science, Tokyo, Japan
[d] Chemical Genetics Laboratory, RIKEN Advanced Science Institute, Saitama, Japan
[e] Biomedicinal Information Research Centre, National Institute of Advance Industrial Science and Technology, Tokyo, Japan
[f] Department of Oncology and Pathology, Cancer Center Karolinska, Karolinska Institutet and Karolinska University Hospital, Stockholm, Sweden

ARTICLE INFO

Article history:
Received 14 May 2012
Available online 23 May 2012

Keywords:
Insulin receptor substrate (IRS)
Deubiquitinating enzyme
Ubiquitin specific protease 7 (USP7)
Degradation
Proteasome
Phosphatidylinositol 3-kinase
Insulin
Insulin-like growth factor (IGF)

ABSTRACT

Insulin receptor substrates (IRSs) play central roles in insulin/insulin-like growth factor (IGF) signaling and mediate a variety of their bioactivities. IRSs are tyrosine-phosphorylated by activated insulin receptor/IGF-I receptor tyrosine kinase in response to insulin/IGF, and are recognized by signaling molecules possessing the SH2 domain such as phosphatidylinositol 3-kinase (PI3K), leading to the activation of downstream pathways. Recent studies have suggested that degradation of IRSs by the ubiquitin–proteasome pathway leads to impaired insulin/IGF signaling, but the precise mechanism underlying the process is still unclear. In this study, we identified deubiquitinating enzyme ubiquitin specific protease 7 (USP7) as an IRS-2-interacting protein and demonstrated that deubiquitinase activity of USP7 plays important roles in IRS-2 stabilization through the ubiquitin–proteasome pathway. In addition, insulin treatment dissociated USP7 from IRS-2, leading to degradation of IRS-2. This dissociation was prevented by treatment with LY294002, a PI3K inhibitor, indicating that insulin activation of the PI3K pathway leads to dissociation of IRS-2 from USP7 and IRS-2 degradation. We obtained similar results for IRS-1 in cells treated with insulin and for IRS-2 in cells treated with IGF-I. Taken together, this is the first report demonstrating that USP7 is an IRS-1/2 deubiquitinating enzyme forming a negative feedback loop in insulin/IGF signaling.

1. Introduction

Insulin stimulates glucose uptake and utilization in muscle and adipose tissues and suppresses glucose production in liver, controlling the maintenance of glucose homeostasis [1]. On the other hand, insulin-like growth factors (IGFs) induce cell proliferation, differentiation and survival of various cell-types, coordinating the growth and development *in vivo* [2]. Insulin receptor substrate (IRS)-1 and IRS-2 are important mediators of insulin/IGF signaling. Tyrosine residues of IRSs are phosphorylated by insulin receptor/IGF-I receptor tyrosine kinase in response to insulin/IGFs, followed by the association with SH2 domain-containing proteins such as phosphatidylinositol 3-kinase (PI3K) and Grb2. These events cause the activation of the downstream kinases such as Akt (also called protein kinase B) and extracellular signal-regulated kinase (Erk), leading to the induction of a variety of insulin/IGF bioactivities [1,2].

Protein levels of IRSs often dramatically change under various conditions such as diabetes [3–6]. Recent studies have shown that several ubiquitin ligases ubiquitinate IRSs and induce their

Abbreviations: IRS, insulin receptor substrate; IGF, insulin-like growth factor; PI3K, phosphatidylinositol 3-kinase; SH2, src homology region 2; USP7, ubiquitin specific protease 7; Grb2, growth factor receptor-bound protein 2; Erk, extracellular signal-regulated kinase; DUB, deubiquitinating enzymes; IRSAP, IRS-associated protein; PVDF, polyvinylidene difluoride; GST, glutathione S-transferase; PMSF, phenylmethylsulfonyl fluoride; KI, kallikrein-inactivating; LC–MS/MS, liquid chromatography–tandem mass spectrometry; MATH, meprin associated TRAF homology; MEK, mitogen-activated protein kinase kinase; CIAP, calf intestinal alkaline phosphatase.

* Corresponding author. Address: Laboratory of Cell Regulation, Departments of Animal Sciences and Applied Biological Chemistry, Graduate School of Agriculture and Life Sciences, The University of Tokyo, 1-1-1 Yayoi, Bunkyo-ku, Tokyo 113-8657, Japan. Fax: +81 3 5841 1311.
E-mail address: atkshin@mail.ecc.u-tokyo.ac.jp (S.-I. Takahashi).

0006-291X/$ - see front matter © 2012 Elsevier Inc. All rights reserved.
http://dx.doi.org/10.1016/j.bbrc.2012.05.093

degradation by the 26 S proteasome [7–10]. In addition, it is well known that prolonged insulin/IGF stimulation induces ubiquitination of IRSs followed by their degradation, which is an important mechanism for the desensitization of insulin/IGF signaling [11,12]. Protein ubiquitination is regulated not only by ubiquitin ligases but also by deubiquitinating enzymes (DUB), however, it is unknown how IRS-1/2 are deubiquitinated.

We have previously shown that IRS-1/2 generally form high-molecular-mass complexes over 1000 kDa containing IRS-associated proteins (IRSAPs) that modulate insulin/IGF signals [13]. In this study, we show that deubiquitinating enzyme USP7 is one of the IRSAPs and it prevents IRS-1/2 ubiquitination and proteasomal degradation. We also demonstrate that insulin or IGF-I treatment stimulates USP7 dissociation from IRSs via activation of PI3K pathway, leading to degradation of IRSs. These results reveal USP7 as an IRS-1/2 deubiquitinating enzyme, forming a negative feedback loop in insulin/IGF signaling.

2. Materials and methods

2.1. Cell culture and reagents

HEK293 cells, HEK293T cells, FRTL-5 thyroid cells, and L6 myoblasts were cultured and transfected as previously described [13–15]. H4IIE hepatoma cells were cultured with Dulbecco's modified Eagle medium containing 10% fetal bovine serum.

2.2. Immunoprecipitation and immunoblotting analysis

These procedures were carried out as described previously [13], except for modifications as described in Supplementary methods.

2.3. LC–MS/MS analysis

LC–MS/MS analysis was performed as described previously [16].

2.4. Purification of GST fused proteins and GST pull-down analysis

These procedures were performed as previously described [17], except for modifications as described in Supplementary methods.

2.5. Far-Western blotting analysis

Proteins were resolved by SDS–PAGE, transferred to polyvinylidene difluoride (PVDF) membranes. After the membranes were incubated with blocking buffer (10 mM Tris–HCl pH 7.2, 50 mM NaCl, 1 mM ethylenediaminetetraacetic acid (EDTA), 3% bovine serum albumin) for 30 min, they were incubated with blocking buffer containing 1 mg/ml GST or GST-fused proteins overnight, followed by the immunoblotting with anti-GST antibody conjugated with horseradish peroxidase.

2.6. Subcellular fractionation into cytoplasm and nuclei

Cells were lysed in fractionation buffer (10 mM Tris–HCl pH 7.4, 100 mM NaCl, 2.5 mM $MgCl_2$, 0.5% TritonX-100, 20 μg/ml calpain inhibitor I (Roche, Basel, Switzerland), 500 μM Na_3VO_4, 10 μg/ml leupeptin, 5 μg/ml pepstatin, 20 μg/ml phenylmethylsulfonyl fluoride (PMSF), and 100 kallikrein-inactivating (KI) U/ml aprotinin). The cell lysates were passed through a 25 G needle syringe four times and centrifuged at 4000*g* for 10 min at 4 °C. The supernatants were saved as the cytoplasmic fraction. The pellets were resuspended in fractionation buffer without TritonX-100, sonicated three times for 5 s, and centrifuged at 15,000*g* for 10 min at 4 °C. The supernatants were saved as the nuclei fraction. The protein assay of the each fractions was performed using a protein assay kit (Bio-Rad Laboratories, Hercules, CA). Equal amounts of proteins subjected to immunoprecipitation and immunoblotting analysis.

2.7. RNA interference

This procedure was performed as previously described [18], except for modifications as described in Supplementary methods.

2.8. In vitro tyrosine phosphorylation and dephosphorylation of IRSs

Phosphorylation/de-phosphorylation of IRSs with insulin receptor kinase/alkaline phosphatase was performed as described in Supplementary methods.

Additional experimental materials and methods are described in Supplementary materials.

3. Results

3.1. USP7 associates with IRS-1/2

In the initial screening to identify IRSs-associated proteins, FLAG-IRS-1 or FLAG-IRS-2 was over-expressed in HEK293 cells, and the cell lysates were subjected to the immunoprecipitation with anti-FLAG antibody-conjugated beads. Mixtures of co-immunoprecipitated proteins were digested with lysyl endopeptidase, and then subjected to LC–MS/MS analysis. As a result, we identified a deubiquitinating enzyme USP7 as one of the IRSs-associated proteins.

Co-immunoprecipitation and immunoblotting analysis validated the initial screening and confirmed that USP7 associated with IRS-1/2 in HEK293T cells over-expressing IRS-1/2 (Fig. 1A and B). We also found that USP7 associated with endogenous IRS-1 and IRS-2 in H4IIE hepatoma cells (Fig. 1C) and in L6 myoblasts (Fig. S1).

We then determined the regions of each protein that are required for their association. Pull-down analysis using USP7 deletion mutants revealed that the MATH domain of USP7 was responsible for the association with IRS-1/2 (Fig. 1D–F). Far-western blotting analysis using the MATH domain of USP7 fused with GST as a probe revealed that this domain directly binds to IRS-1/2 (Fig. 1G). On the other hand, pull-down analysis using IRS-1/2 deletion mutants indicated that USP7 binds to multiple regions in IRS-1/2 (Figs. S2A and B). We also investigated the subcellular localization of USP7-IRS-2 complex. Co-immunoprecipitation analysis after subcellular fractionation into cytoplasm and nuclei indicated that a large part of the complex is detected in the cytoplasm in H4IIE cells (Fig. 1H).

3.2. USP7 deubiquitinates IRS-2 and prevents its proteasomal degradation

We next investigated the physiological roles of USP7 for IRS-2. We hypothesized that USP7 deubiquitinates IRS-1/2 and prevents their proteasomal degradation. In HEK293 cells, over-expression of USP7 resulted in the increase in IRS-2 protein levels (Fig. 2A). By contrast, over-expression of dominant negative USP7 (USP7 CS, where the single cysteine residue in the catalytic center was substituted with serine [19]) decreased IRS-2 protein levels, an effect prevented by pre-treatment with a proteasome inhibitor MG132 (Fig. 2B, left panel). Importantly, over-expression of dominant negative USP7 CS increased ubiquitination of IRS-2 in the presence of MG132 (Fig. 2B, right panel). Moreover, in H4IIE cells,

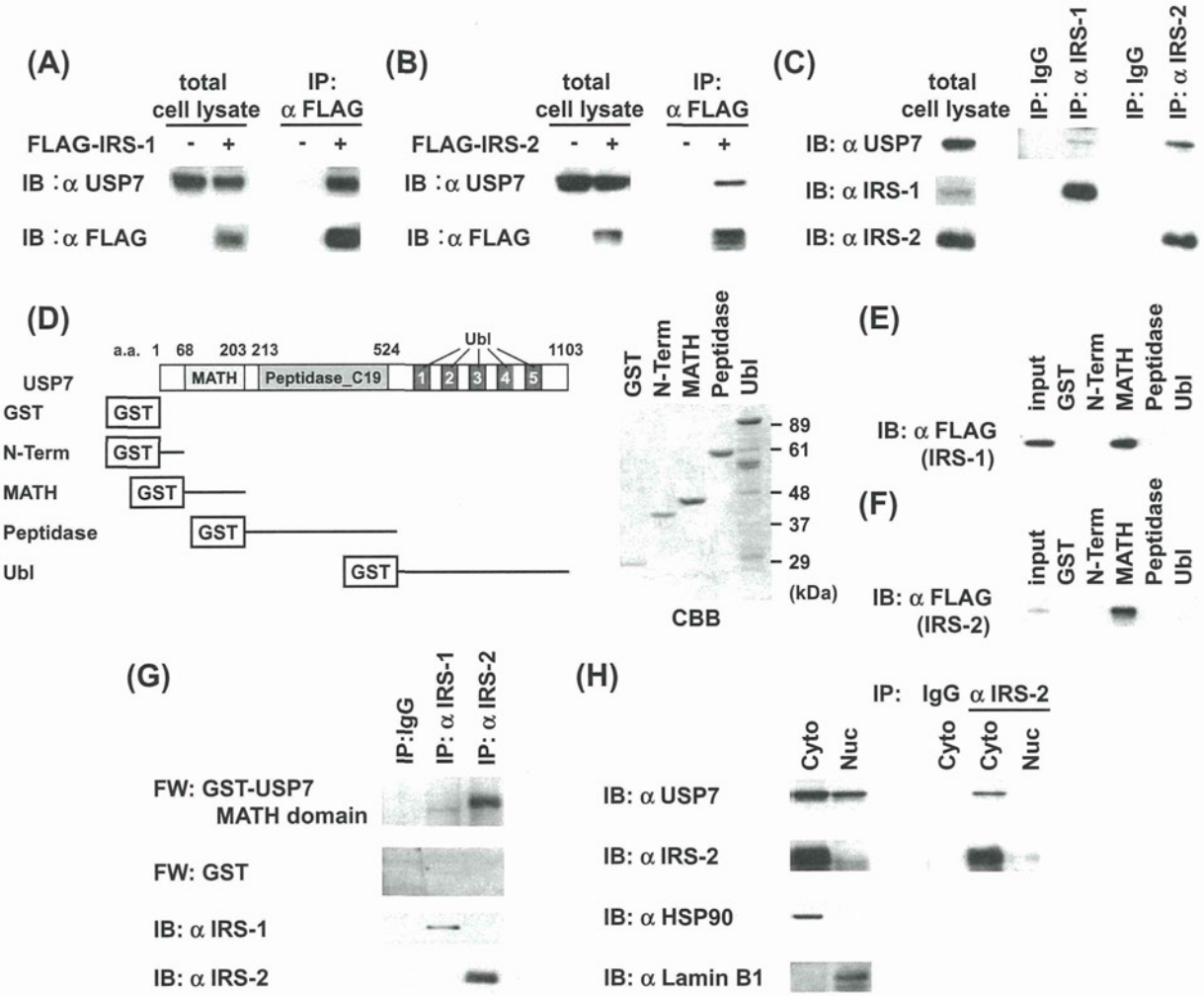

Fig. 1. The association of USP7 with IRS-1/2. (A–C) HEK293T cells over-expressing FLAG-IRS-1 (A) or FLAG-IRS-2 (B), or H4IIE cells (C) were cultured under serum-free conditions for 24 h. The lysates were subjected to immunoprecipitation (IP) and immunoblotting (IB) analyses. (D) Schematic representation of rat USP7 and its deletion mutants used in the following experiments. MATH, meprin associated TRAF homology domain. Ubl, ubiquitin-like domain. The purity of GST-fused proteins was validated by CBB staining. (E and F) HEK293T cells over-expressing FLAG-IRS-1 (E) of FLAG-IRS-2 (F) were cultured under serum-free condition for 24 h. The lysates were subjected to pull-down analysis using GST-fused USP7 deletion mutants. Input, 3/100 volume of HEK293T cell lysates. (G) Lysates of serum-starved H4IIE cells were immunoprecipitated with anti-IRS-1/2 antibodies. The immunoprecipitates were resolved by SDS–PAGE and subjected to far- western blotting (FW) analyses using purified GST or GST-fused MATH domain of USP7 (upper panels) as probes, and immunoblotting analysis using anti-IRS-1/2 antibodies (lower panels). (H) Lysates of serum-starved H4IIE cells were fractionated into cytoplasm (Cyto) and nuclei (Nuc), followed by immunoprecipitation with anti-IRS-2 antibody. The fractions and immunoprecipitates were subjected to immunoblotting analysis. Lamin B1, a nuclear protein. HSP90, a cytoplasmic protein. Data are representative of at least three independent experiments.

knockdown of USP7 decreased IRS-2 protein levels (Fig. 2C). All of these results support our hypothesis that USP7 prevents IRS-2 degradation by deubiquitinating activity. In addition, we found that over-expression of dominant-negative USP7 CS decreased IRS-1 protein levels (Fig. 2D), indicating that USP7 also plays roles in the regulation of IRS-1 protein levels.

3.3. USP7 dissociates from IRS-1/2 in response to insulin/IGF stimulation, leading to the proteasomal degradation of IRS-1/2

In several cell-types, insulin/IGF stimulation causes the association of some ubiquitin ligases with IRS-1/2, followed by their proteasomal degradation [7,8,10], which is thought to be one of the feedback inhibition mechanisms in insulin/IGF signaling [7,8,10,11]. We examined the effects of insulin stimulation on the association of USP7 with IRS-2 in H4IIE cells. Surprisingly, co-immunoprecipitation analysis revealed that the amounts of USP7 bound to IRS-2 were dramatically decreased within 1 min after insulin stimulation (Fig. 3A). We also found that insulin stimulation gradually decreased electrophoretic mobility of IRS-2 at 1–60 min after insulin stimulation reflecting its phosphorylation state [20] followed by the decrease in IRS-2 protein levels (Fig. 3A). In addition, we found that USP7 also dissociated from IRS-1 in response to insulin stimulation followed by decrease of IRS-1 protein levels (Fig. 3B). In FRTL-5 cells, IGF-I stimulation dissociated USP7 from IRS-2 followed by decrease of IRS-2 protein levels (Fig. 3C). These results clearly indicate that the rapid dissociation of USP7 from IRS-1/2 in response to insulin/IGF-I stimulation may enable the subsequent ubiquitination and proteasomal degradation of IRS-1/2.

3.4. USP7 dissociates from IRS-2 followed by its degradation through activation of the PI3K pathway in response to insulin stimulation

Finally, we investigated molecular mechanisms of the USP7 dissociation. Insulin-induced dissociation was prevented in the presence of LY294002, a PI3K inhibitor, but not of PD98059, a MEK inhibitor (Fig. 4A and B). We also performed pull-down analysis using the MATH domain of USP7 as a bait and IRS-2 derived from H4IIE cells treated with or without insulin as a prey. The result

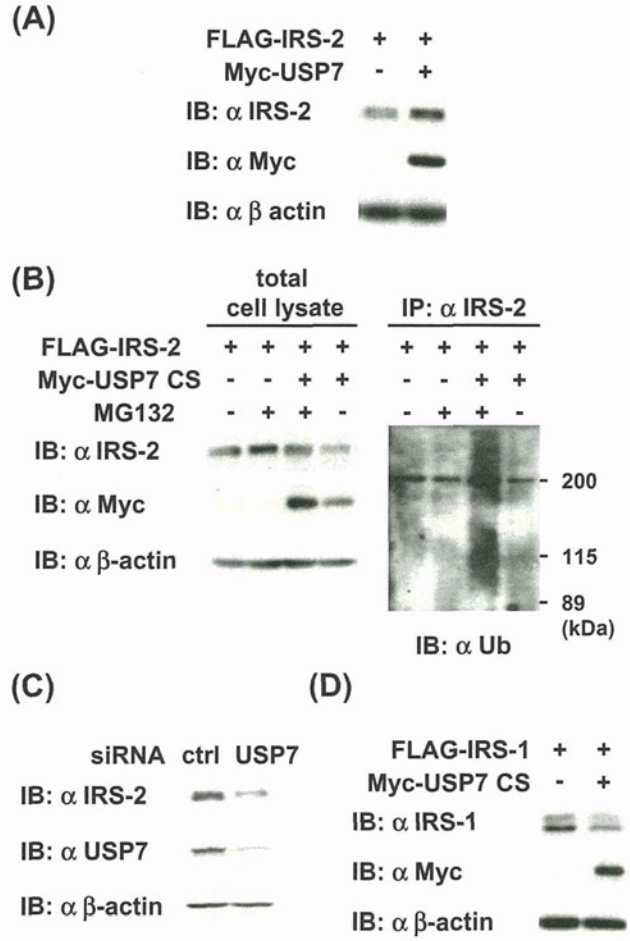

Fig. 2. Roles of USP7 in the regulation of IRS-1/2 protein levels. (A) HEK293 cells over-expressing indicated proteins were cultured under serum-free condition for 24 h. The cell lysates subjected to immunoblotting analysis. β-Actin, loading control. (B) HEK293 cells over-expressing FLAG-IRS-2 and myc-USP7 CS (dominant-negative mutant) were cultured under serum-free condition for 24 h, and treated with 10 μM MG132 for the last 6 h. The lysates were subjected to immunoprecipitation and immunoblotting analysis. (C) H4IIE cells transfected with control RNA or USP7 siRNA were cultured under serum-free condition for 24 h. The lysates were subjected to immunoblotting analysis. (D) HEK293 cells over-expressing FLAG-IRS-1 and myc-USP7 CS were cultured under serum-free condition for 24 h. The lysates were subjected to immunoprecipitation and immunoblotting analysis. Data are representative of at least three independent experiments.

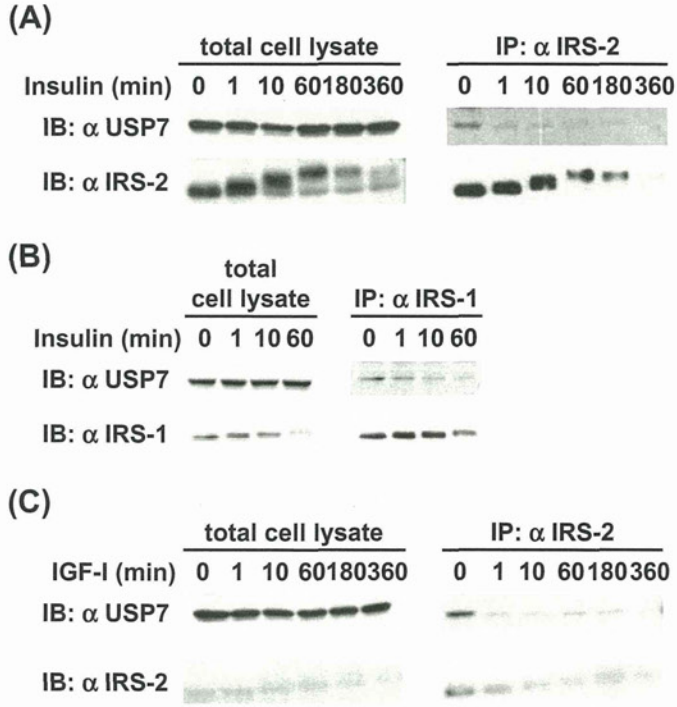

Fig. 3. The dissociation of USP7 from IRS-1/2 in response to insulin/IGF stimulation. (A–C) Serum-starved H4IIE cells (A and B) or FRTL-5 cells (C) were treated with 100 nM insulin (A and B) or 100 ng/ml IGF-I (C) for the indicated durations. The lysates were subjected to immunoprecipitation with anti-IRS-1 antibody (B) or anti-IRS-2 antibody (A and C) and immunoblotting analysis.

indicated that insulin stimulation decreased the affinity of IRS-2 for the MATH domain, and this decrease was prevented by the treatment of cells with LY294002 (Fig. 4C), suggesting that phosphorylation of IRS-2 via PI3K pathway triggers the USP7 dissociation.

IRS-2 is phosphorylated by some serine/threonine kinases downstream of PI3K [21]. To examine the roles of the serine/threonine phosphorylation of IRS-2 in the association with the MATH domain, IRS-2 derived from cells stimulated with serum was treated with alkaline phosphatase *in vitro*, and then subjected to the pull-down analysis. The result indicated that phosphorylation of IRS-2 decreased the affinity of IRS-2 for the MATH domain (Fig. 4D). In contrast, tyrosine phosphorylation of IRS-2 by insulin receptor kinase *in vitro* prior to the pull down analysis did not affect the affinity of IRS-2 for the MATH domain (Fig. 4E).

4. Discussion

In this study, we identified deubiquitinating enzyme USP7 as an IRSs-associated protein and examined the physiological significance of this association in the regulation of insulin/IGF signaling. Based on our results, USP7 deubiquitinated IRS-1/2 resulting in increase in their stabilization. In addition, insulin/IGF treatment caused dissociation of USP7 from IRS-1/2 followed by induction of their degradation, suggesting that USP7 formed a negative feedback loop in insulin/IGF signaling.

Since the human genome encodes 95 different DUBs [22], many fewer than the more than 600 E3 ligase molecular species [23], DUBs are considered to be low specificity enzymes. Actually, numerous proteins have been identified as potential substrates of USP7 [24] including p53, a tumor suppressor, and Mdm2, an E3 ligase of p53 [19,25]. USP7 associates with these proteins through the MATH domain and deubiquitinates them [26,27]. In addition, USP7 regulates these protein levels through alteration of affinity for these proteins [28] and phosphorylation of serine residues within the MATH domain-binding motif of p53 or Mdm2 which abrogated binding to USP7 [29]. We demonstrated that USP7 directly associated with IRS-2 through the MATH domain (Fig. 1G), and that dephosphorylation of IRS-2 increases the interaction while tyrosine phosphorylation of IRS-2 by insulin receptor kinase did not increase the interaction (Fig. 4D and E), suggesting the common mechanisms for IRS-2 and p53/Mdm2 that serine/threonine phosphorylation of their binding regions reduces their USP7 association. Different phosphorylation status of each substrate may enable USP7 to regulate their protein stabilities specifically.

Recent studies have shown that several serine/threonine kinases downstream of PI3K such as Akt, GSK-3, mTOR and p70S6K phosphorylate IRS-1/2, and the phosphorylation triggers IRS-1/2 ubiquitination and degradation [21]. In addition, particular serine residues of IRS-1 such as S307, S527, S636 and S639 were reported to be key phosphorylation sites required for IRS-1 degradation [8,21]. In the present study we demonstrated that IRS-2 modification induced by insulin stimulation via PI3K pathway activation releases USP7 from IRS-2 (Fig. 4B). Taken together with the data